SAMSO-TR-69-29

OSCILLATOR STRENGTHS OF TRANSITIONS BETWEEN RYDBERG STATES OF NITRIC OXIDE IN THE NEAR IR

Kurt L. Wray

AVCO EVERETT RESEARCH LABORATORY

RESEARCH REPORT 300
FEBRUARY 1969

jointly sponsored by
ADVANCED RESEARCH PROJECTS AGENCY
DEPARTMENT OF DEFENSE
ARPA Order No. 1092
and
SPACE AND MISSILE SYSTEMS ORGANIZATION
AIR FORCE SYSTEMS COMMAND
DEPUTY FOR RE-ENTRY SYSTEMS (SMY)
Norton Air Force Base, California 9240[illegible]

58

BLANK PAGES
IN THIS
DOCUMENT
WERE NOT
FILMED

SAMSO-TR-69-29 RESEARCH REPORT 300

OSCILLATOR STRENGTHS OF TRANSITIONS BETWEEN RYDBERG STATES OF NITRIC OXIDE IN THE NEAR IR*†

by

Kurt L. Wray

February 1969

AVCO EVERETT RESEARCH LABORATORY
a division of
AVCO CORPORATION
Everett, Massachusetts

*This research was supported by the Advanced Research Projects Agency of the Department of Defense and Space and Missile Systems Organization, Air Force Systems Command and was monitored by Space and Missile Systems Organization, Air Force Systems Command under Contract F04701-68-C-0036.

†Submitted to J. Q. S. R. T. Journal

FOREWORD

"This research was supported by the Advanced Research Projects Agency of the Department of Defense and Space and Missile Systems Organization, Air Force Systems Command and was monitored by Space and Missile Systems Organization, Air Force Systems Command under Contract F04701-68-C-0036." The secondary report number as assigned by AERL is Avco Everett Research Report 300, and the author is Kurt L. Wray. The Air Force program monitor for this contract is T.W. Graham, 2nd Lt., USAF, Project Officer, Environmental Technology Branch, SMYSE.

Publication of this report does not constitute Air Force approval of the report's findings or conclusions; it is published only for the exchange and stimulation of ideas.

T.W. Graham, 2nd Lt., USAF,
Project Officer,
Environmental Technology Branch,
SMYSE

ABSTRACT

In recent years several shock tube studies have been made of the radiation emanating from hot air and nitrogen in the near IR. These investigations showed about 10 times more radiation from air than could be accounted for on the basis of the $N_2(1+)$ band system alone; however, there has been some controversy as to the source of this excess air radiation. The present experiments utilized a continuously running 1 atm constricted arc jet to prepare equilibrium air and nitrogen at temperatures between 3500 and 5800°K. The excess air radiation was confirmed, and it was shown that it requires the presence of both N and O nuclei. High resolution spectra (13 Å) were obtained from .9 to 1.2 μ employing a scanning monochromator and photomultiplier. Most of the features of these air spectra could be correlated with transitions arising between Rydberg states of NO. Employing the available spectroscopic parameters, theoretical calculations of the wavelength dependence of the radiation were made. By comparing the calculated total synthetic spectra with the experimental spectra, f-numbers for nine NO Rydberg systems have been evaluated.

TABLE OF CONTENTS

		Page
	Foreword	ii
	Abstract	iii
	List of Illustrations	vii
I.	INTRODUCTION	1
II.	EXPERIMENTAL TECHNIQUE	3
III.	EXPERIMENTAL RESULTS	9
IV.	THEORETICAL MODEL	19
V.	COMPARISON OF THEORY AND EXPERIMENT	33
VI.	DISCUSSION	45
VII.	ACKNOWLEDGMENTS	51
	REFERENCES	53

LIST OF ILLUSTRATIONS

Figure		Page
1	Schematic diagram of arc used to obtain high temperature air.	4
2	Schematic diagram of high wavelength resolution IR arc radiation monitoring system.	6
3	Radiation intensity from arc heated air as a function of arc energy balance temperature at a wavelength of 1.0382μ	10
4	Comparison of arc heated air and nitrogen photographic spectra in the 1μ region.	11
5	Wavelength scan of arc heated air.	13
6	Experimentally determined radiation intensity from hot air plotted against wavelength in the 1μ region.	15
7	CN red system spectrum obtained from arc heated nitrogen containing a "trace" of C_2H_6.	17
8	Potential energy diagram for nitric oxide showing the various electronically excited states of interest in this study.	20
9	Theoretically computed radiation intensity per partical as a function of wavelength for the nitric oxide Rydberg transitions (a) M → C and (b) K → C at T = 5700°K.	26
10	Theoretically computed radiation intensity per partical as a function of wavelength for the nitric oxide Rydberg transitions (a) M → D and (b) K → D at T = 5700°K.	27
11	Theoretically computed radiation intensity per partical as a function of wavelength for the nitric oxide Rydberg transitions (a) H' → C and (b) H → C at T = 5700°K.	28
12	Theoretically computed radiation intensity per partical as a function of wavelength for the nitric oxide Rydberg transitions (a) F → C and (b) H' → D at T = 5700°K.	29
13	Theoretically computed radiation intensity per partical as a function of wavelength for the nitric oxide Rydberg transitions (a) H → D and (b) D → A at T = 5700°K.	30

Figure		Page
14	Theoretically computed radiation intensity per partical as a function of wavelength for the nitric oxide Rydberg transitions (a) E → C and (B) C → A at T = 5700°K.	31
15	Comparison of the theoretically computed spectral intensity from air at T = 5700°K with the experimental results.	38
16	Comparison of the theoretically computed spectral intensity from air at T = 5800°K with the experimental results.	39
17	Comparison of the theoretically computed spectral intensity from air at T = 6300°K and 6500°K with the shock tube data of Wurster, et al.[2,7]	44

LIST OF TABLES

Table		Page
I	Relative Energies and Rotational Constants of the Ten Lowest Lying Rydberg States of Nitric Oxide	21
II	Computed Band Origins for Transitions Between the Ten Lowest Lying Rydberg States of Nitric Oxide	22
III	Equilibrium Concentrations in Particles per cc and Rydberg System Radiation Correction Factors to Account for Omission of States $v' \geq 2$	34
IV	Experimentally Determined Oscillator Strengths for Transitions Between Rydberg States of Nitric Oxide in the Wavelength Region 0.9 to 1.2 Microns	37
V	Comparison of Theoretical and Experimental Atomic Line Intensities at T = 5690°K.	42

I. INTRODUCTION

In recent years numerous shock tube studies have been made of the radiation emanating from hot air and nitrogen in the near IR portion of the spectrum.[1-7] All of these investigations concur in that the measured radiation from air is about a factor of 10 more intense than one can account for on the basis of the $N_2(1+)$ band system alone. However, a controversy has arisen as to the source of this "excess" air radiation. The work of Wurster, Treanor and Thompson,[2] in which the radiation was monitored behind reflected shock waves in air and various O_2-N_2 mixtures, indicated that the excess radiation scaled like the NO concentration in the equilibrium gas behind the reflected shock. In their work a multichannel monochromator was employed and some wavelength resolution of the radiation was obtained. Their data and conclusions have been extensively reviewed by Keck, et al[8] who found the evidence for the NO band hypotheses not completely convincing.

In a previous shock tube study employing incident shock waves in both nitrogen and air, Wray and Connolly[6] agreed with the amount of excess air radiation found by Wurster. However, the scaling was found not to agree with the nitric oxide hypothesis, but indeed the radiation seemed to scale better with nitrogen concentration. Furthermore in that paper it was argued that the absolute intensity of the excess air radiation would demand an oscillator strength significantly larger than unity for the nitric oxide band hypothesized.

There were two reasons for carrying out the present work; the first was that some question arose as to whether the measurements previously made[6] behind incident shocks were valid due to the possible lack of attainment of equilibrium at the lowest densities studied. Indeed, comparisons were made of the computed time history of the relaxation behind incident shocks in air with the radiation oscillograms. It was learned that for the low initial pressure cases, at low temperatures, the radiation records were read at a time when the gas had not yet relaxed to equilibrium. The traces "looked flat" because the chemical relaxation process was very slow. Since both the NO concentration and the temperature are decreasing as equilibrium is approached, the radiation measured was larger than it would have been at true equilibrium. Indeed, in a recent paper Wurster and Marrone[7] have raised exactly this question relative to the validity of our early work.

The second reason for the present work is that high resolution spectral data could be obtained on the 1 atmosphere continuously running high temperature arc facility at our Laboratory. As will be described below, this facility was used to take detailed spectra from 0.90 to 1.20 μ of equilibrium air at temperatures between 3500 and 5800°K. The conclusions drawn from these spectra are that the source of the excess air radiation is nitric oxide, and because of the nature of the spectral distribution in these particular band systems, the measured intensities lead to reasonable oscillator strengths.

II. EXPERIMENTAL TECHNIQUE

The arc facility which was employed in obtaining the new experimental results to be given below is described in detail in Refs. 9 and 10. A schematic drawing of this apparatus is shown in Fig. 1. All internal components of the arc (which is about 30 cm long) are constructed of copper except for the tungsten tipped cathode. The arc is started by means of a capacitor discharge across the gap between cathode and anode at (E) and is "blown" downstream by the N_2 flow to a position giving stable arc operation. The total electrical power put into the arc is increased in steps by switching in individual (water cooled) resistors in parallel, thus reducing the ballast resistance which is in series with the battery bank power supply and the arc. The gas power is calculated by subtracting the wall losses from the arc power, the losses being obtained by measuring the temperature rise and the flow rate of the coolant water flowing in cavities (G). Typical operating conditions are as follows: at a total arc power of 330 kW and an air mass flow rate of 22×10^{-3} lbs/sec, an arc efficiency of 38.3% was calculated, the equilibrium air temperature being $5590^{\circ}K$.

The hot air exits into the atmosphere where spectroscopic studies can be made within 1 mm of the 1.9 cm diameter exit nozzle. The synthetic air (containing just N_2 and O_2 in the proper ratio) was shown to be in equilibrium in previous work.[9,10] References 9 and 10 describe, in part, absolute radiation measurements obtained from arc-heated air

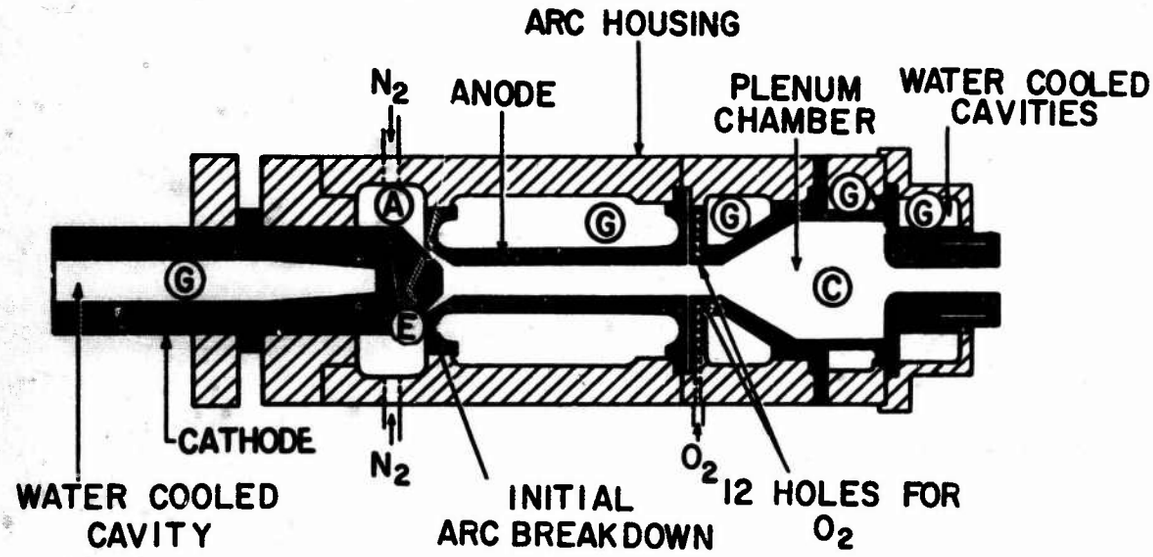

Fig. 1 Schematic diagram of arc used to obtain high temperature air. N_2 is introduced tangential to cathode at (A). O_2 is introduced downstream through twelve holes and mixing occurs in plenum chamber (C).

A3656X

at a wavelength of 3869 Å. These compared well with theoretical predictions which included contributions from O^- (free bound), C_2 (Schumann-Runge) $N_2^+(1-)$, $N_2(2+)$ and NO(β). For the band pass employed, the NO(β) radiation dominated between 4100 and 6000°K. Furthermore, intensity measurements[11] of the NO vibration-rotation fundamental band at 5.3μ made on arc heated air yielded a value of 120 cm^{-2} atm^{-1} for the integrated intensity, this being in excellent agreement with recent literature values of 115[12] and 124[13] cm^{-2} atm^{-1}. These measurements, both in the visible and IR, confirm the presence of equilibrium amounts of NO in the arc heated air at the energy balance temperature. Unfortunately, the temperature of the arc heated air is not uniform in time, but has random high frequency (~ 10^5 cps) fluctuations of the order of several hundred degrees.[9] This makes the arc apparatus unsuitable for extremely accurate quantitative experiments, but, because of its continuous operation, the device is most useful for obtaining spectra such as will be discussed below.

In the present study, spectra were obtained using two different instruments, the speed of both being limited by an f/12 external mirror optical system (see Fig. 2). Spectra were recorded photographically using a Hilger glass prism spectrograph employing Kodak Z film hypersensitized with ammonium hydroxide. The dispersion of this instrument in the vicinity of 1μ was about 200 Å per mm. Higher resolution spectra were obtained with a Bausch and Lomb grating monochromator with a dispersion of 33 Å per mm, the slits being adjusted in this experiment to yield a spectral resolution (width at half height) of

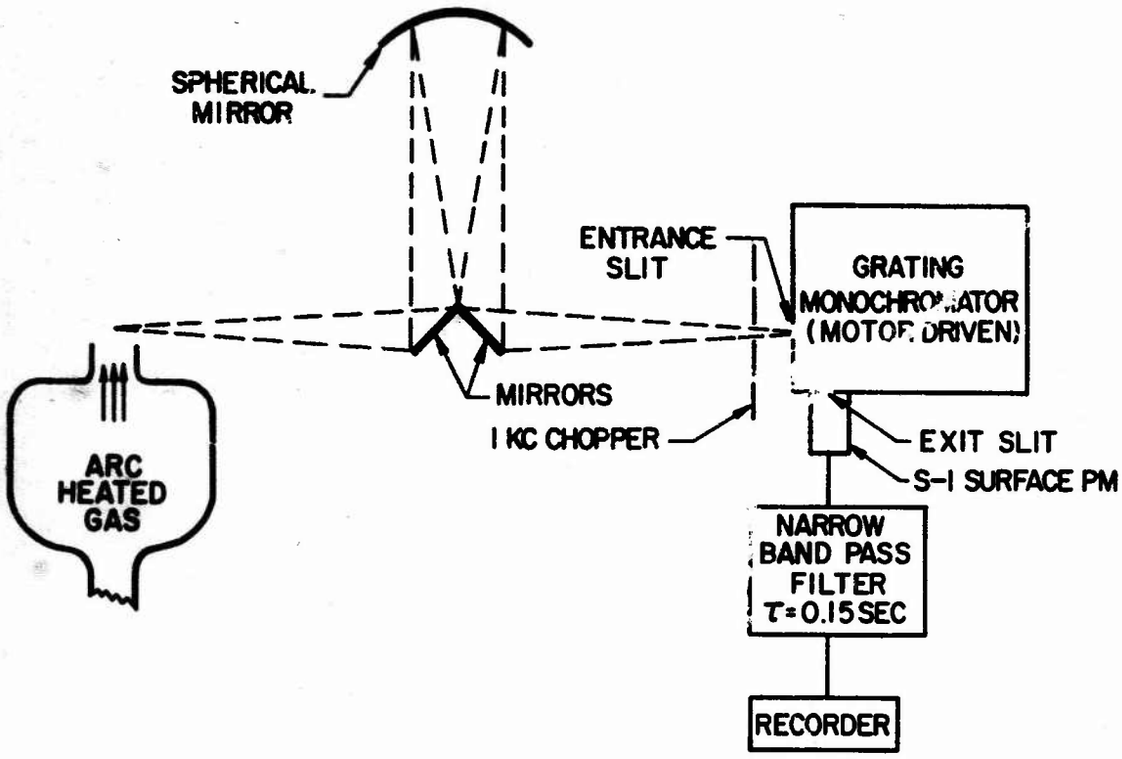

Fig. 2 Schematic diagram of high wavelength resolution IR arc radiation monitoring system.

A7816

13 Å. The system is shown schematically in Fig. 2. The dispersed radiation from the Bausch and Lomb was detected using a dry ice cooled S-1 photocathode photomultiplier. The light was chopped at about 1000 cycles per second before entering the instrument and the photomultiplier output was monitored on a Visicord recorder after passing through a 10 cycle band pass filter centered on the chopping frequency and averaged for a time $\tau = 0.15$ sec. The wavelength was varied continuously by a motor drive, 90 seconds being required to scan from 0.9 to 1.20μ.

The Bausch and Lomb instrument was also employed to make some absolute intensity measurements at a fixed wavelength of 1.0382μ, with a band pass (width at half height) equal to 33 Å. This instrument with the same slit settings was employed in the previous study,[6] and the present measurements can be compared directly with those shock tube data.

In identifying the high temperature equilibrium spectrum obtained with the Hilger spectrograph, numerous spectra were taken using the same instrument but employing as a light source condensed and uncondensed discharges in various gases. The apparatus employed to make these discharges consisted simply of a small cylindrical plexiglass chamber through which the gas to be studied was flowed at a pressure of 1 atmosphere. The discharge was made between two 6 mm diameter stainless steel, chisel pointed electrodes spaced approximately 1 mm apart. A high voltage discharge was made across these electrodes. An optical grade glass window permitted the light emanating from the discharge to be focused on the entrance slit of the Hilger instrument.

III. EXPERIMENTAL RESULTS

Figure 3 shows the absolute radiation intensity from air obtained at a fixed wavelength of 1.0382μ as a function of temperature (i.e., the energy balance temperature in the arc heated synthetic air). Also shown on this figure is the theoretically computed radiation[6] due to the $N_2(1+)$ band system based on an oscillator strength of 3.38×10^{-3},[6] and a small contribution due to the NO + O continuum based on the rate constant and spectral distribution given by Wurster and Marrone.[15] It is clear that the excess air radiation is again confirmed. In fact, at the highest temperatures studied, where the effect of the arc fluctuations are rather insignificant, the excess air radiation is in agreement with the factor 7 obtained in the earlier work.[6] To make the comparison more quantitative, in Ref. 6 data are given showing an intensity of 1.05×10^{-1} watts/cm^3-ster-μ at T = 5700°K for an initial shock tube pressure of 5 torr. These conditions correspond to an equilibrium NO concentration of 3.1×10^{16}/cm^3. Equilibrium arc conditions (P = 1 atm, T = 5700°K) correspond to [NO] = 1.34×10^{16}/cm^3; hence, an intensity of 4.5×10^{-2} watts/cm^3-ster-μ is predicted for the arc if the radiation is assumed proportional to the NO concentration. This is in excellent agreement with the arc data as can be seen in Fig. 3.

An example of the 1μ region spectra obtained on the Hilger instrument for both air and nitrogen is shown in Fig. 4 where the excess radiation in the vicinity of 1.04μ is clearly seen. Note that the $N_2(1+)0,0$

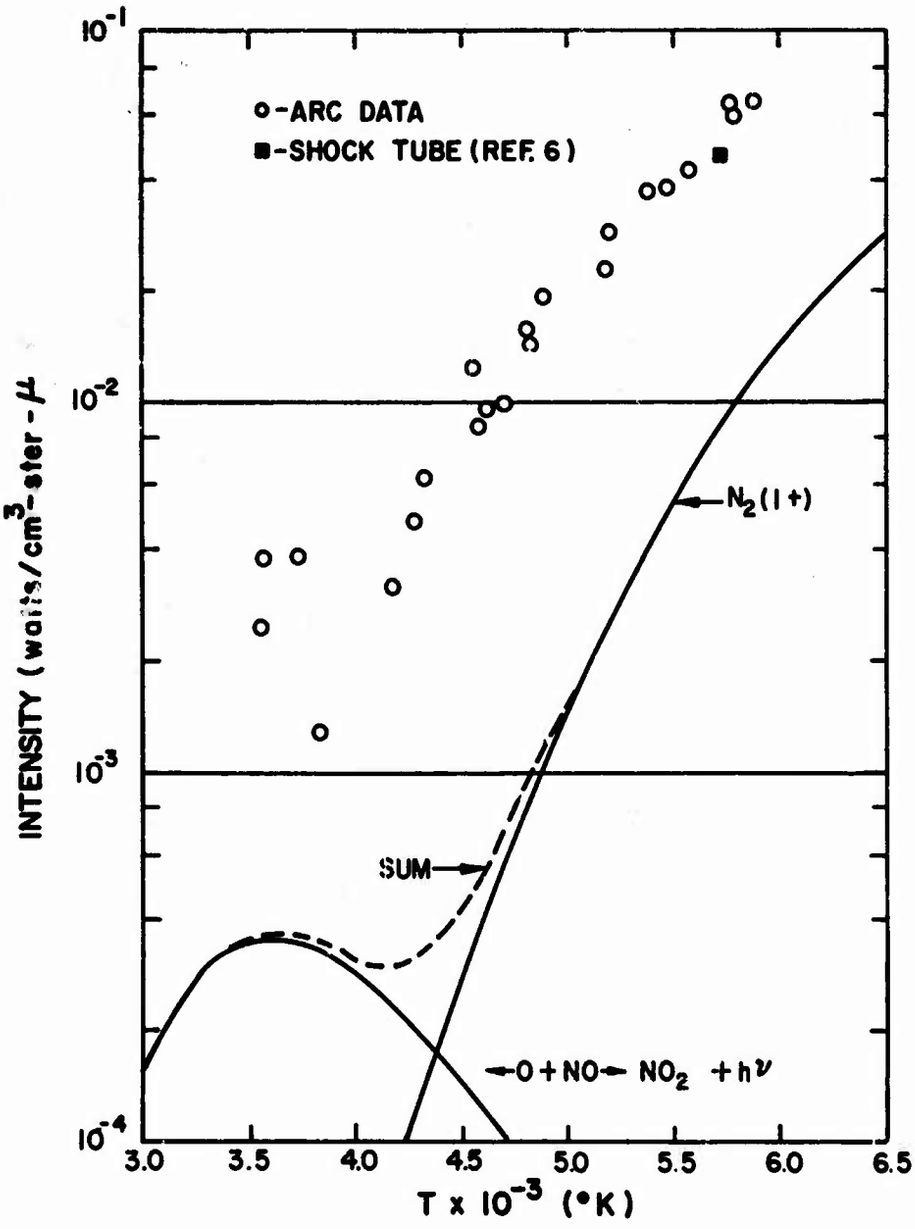

Fig. 3 Radiation intensity from arc heated air as a function of arc energy balance temperature at a wavelength of 1.0382 μ. The band pass (width at half height) is 33 Å.

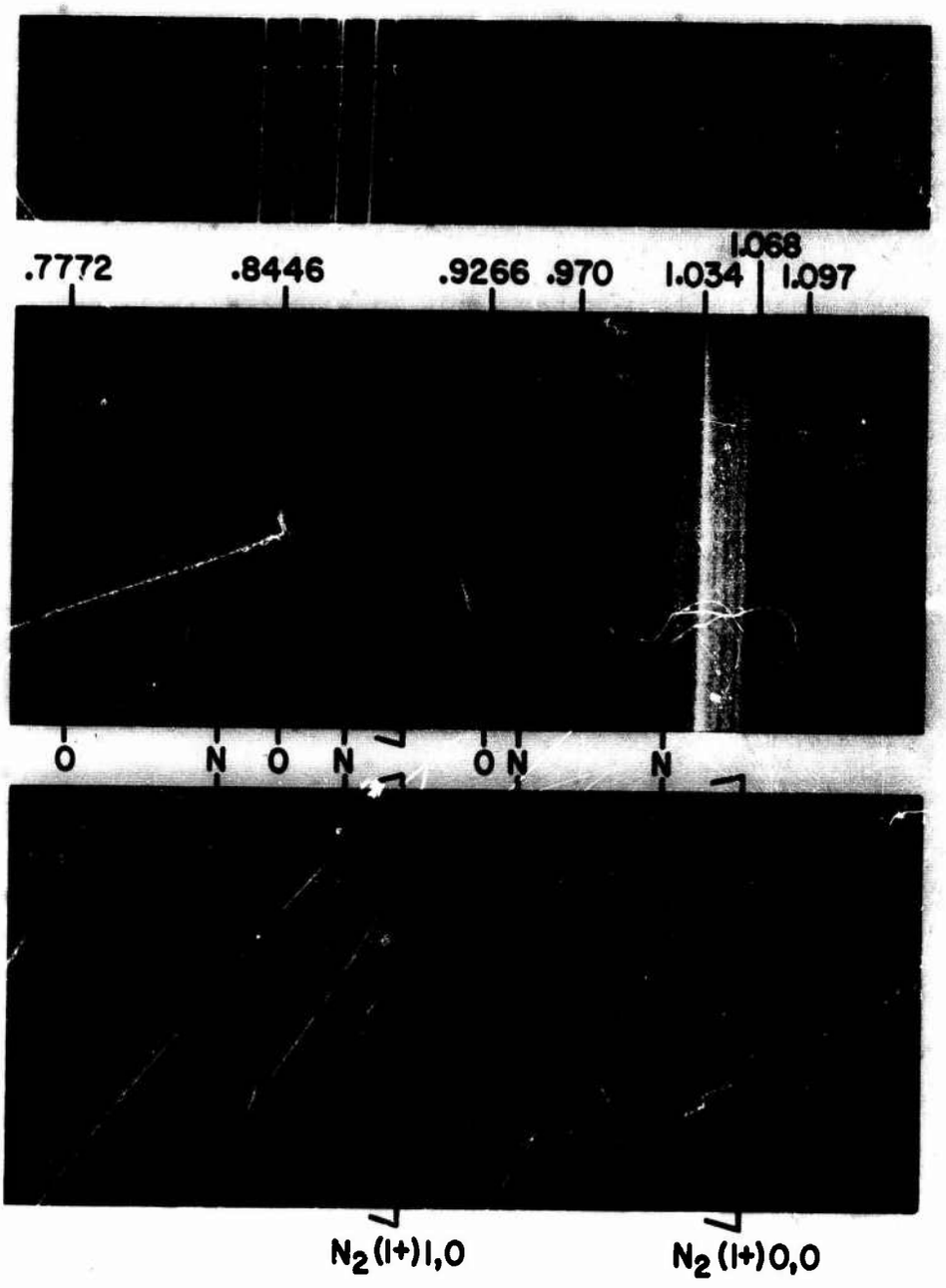

Fig. 4 Top spectrum: Neon geissler tube for wavelength calibration. Middle spectrum: Arc heated air, energy balance temperature equals 5690°K, exposure equals 100 seconds. Bottom spectrum: Arc heated nitrogen, energy balance temperature equals 5680°K exposure equals 100 seconds. The entrance slit to the spectrograph was 25 μ for all three spectra.

band is seen in the nitrogen but is completely masked in the air spectra by the radiation of interest. On the other hand, the 1, 0 band at 8912 Å is seen for both nitrogen and air. Various features of interest in the spectrum are called out.

The experiments performed with the discharge light source described above clearly proved that the dominant features of the air spectrum shown in Fig. 4 require the presence of both nitrogen and oxygen nuclei. Spectra essentially identical with that shown for air were obtained in the uncondensed discharge when either air or nitric oxide were employed in the discharge. On the other hand, spectra taken of O_2, N_2, NH_3, CO_2, C_2H_6, and $C_2H_6 + N_2$ showed no correlation with the air spectra of Fig. 4.

In Fig. 5 we show a portion of the high resolution spectra obtained with the scanning monochromator. Three atomic lines are indicated, two of which are also seen in the spectrogram of Fig. 4. It should be pointed out that Fig. 5 shows raw data and that the wavelength sensitivity of the photomultiplier must be folded in to get relative intensities.

Twelve high resolution spectra, similar to that shown in Fig. 5, have been analyzed yielding plots of the absolute intensity as a function of wavelength. This was carried out in the following manner. The Visicord recordings were read point by point on an Oscar, enough x, y coordinates being taken to completely reproduce the spectral details. Similar readings were taken of a Visicord trace produced by scanning a calibrated black body source over the same wavelength interval. The spectral scans of the high temperature air showed three atomic lines

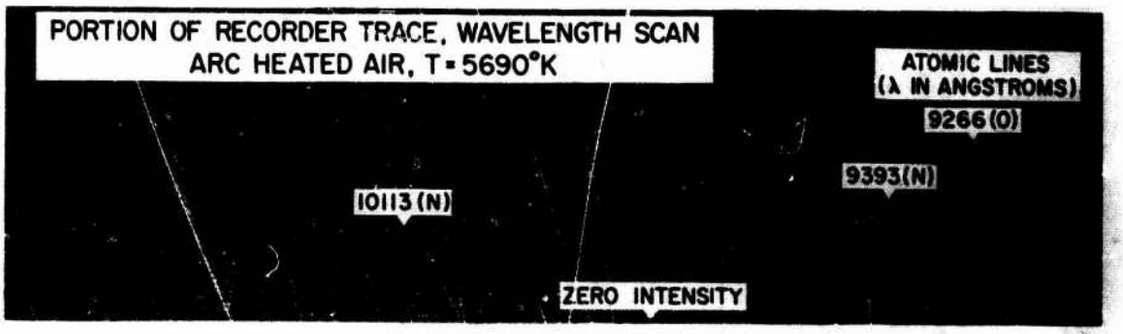

Fig. 5 Wavelength scan of arc heated air. Energy balance temperature equals 5690°K. Spectral resolution (width at half height) is 13 Å.

corresponding to the oxygen line at 9266 Å and nitrogen lines at 9393 and 10113 Å. These three spectral features served as an internal wavelength standard in each run and were used to convert the x coordinate in arbitrary units into absolute wavelength.

A computer program was written which utilized the x, y coordinates of the air spectrum and the black body scan along with the x coordinates of the above three mentioned atomic lines to compute the absolute intensity spectrum. The calculated spectra were plotted directly from the computer tapes. Figure 6 shows four such spectra at arc energy balance temperatures of 3400, 4550, 5690, and 5800°K. Comparison of these spectra show the high degree of reproducibility of the spectral details. At the lower temperatures at wavelengths beyond about 1.15μ, the signal to noise ratio becomes extremely poor due to the loss of sensitivity of the S-1 photomultiplier surface in this wavelength regime.

Due to this rapidly decreasing sensitivity, the amplitude of the signals became objectionally small at the longer wavelengths if the gain settings were such that the shorter wavelength portions of the trace were on scale. Two runs at slightly higher temperatures were made at longer wavelengths with the gain being adjusted stepwise throughout the run (and calibration) so as to overcome this difficulty. One of these is the bottom spectra in Fig. 6.

It had been suggested that perhaps some of the excess radiation was due to the CN red system, in some unknown way enhanced by the presence of oxygen. In any case, impurity radiation has often interferred with spectral measurements and it was deemed advisable to deliberately

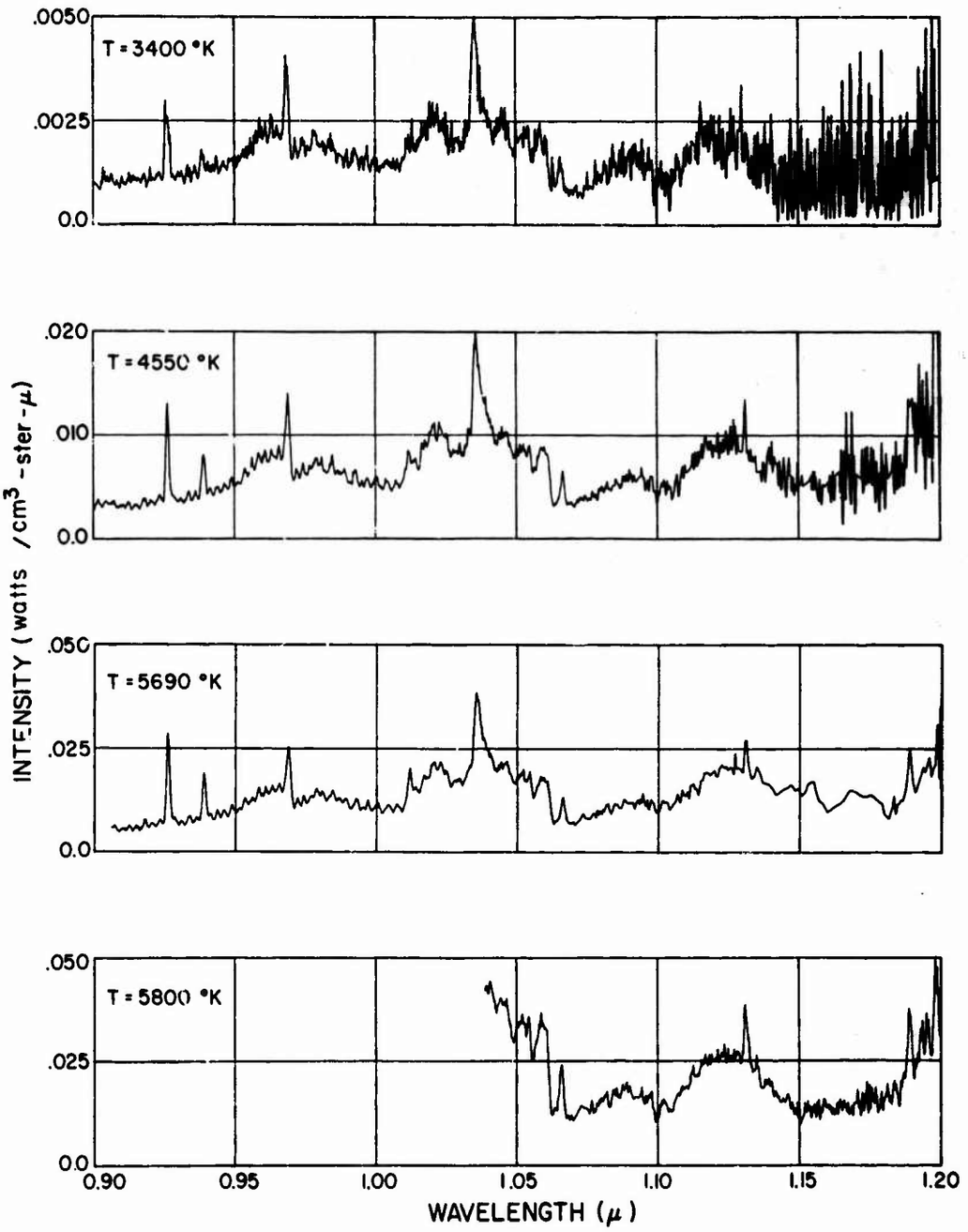

Fig. 6 Experimentally determined radiation intensity from hot air plotted against wavelength in the 1 μ region. The spectral resolution (width at half height) was 13 Å. Note the high degree of reproducibility of the spectral details at the four temperatures shown.

obtain a carbon contaminated spectrum in the present work for comparison purposes. The spectrum shown in Fig. 7 was obtained from the radiation emanating from arc heated nitrogen containing a "trace" of ethane; it displays the 0, 0 and 1, 0 bands of the CN red system. The "multiheaded" structure of these bands[16] is clearly seen. Comparison of Fig. 7 with Fig. 6 shows that this radiation does not make a significant contribution to the spectra under study.

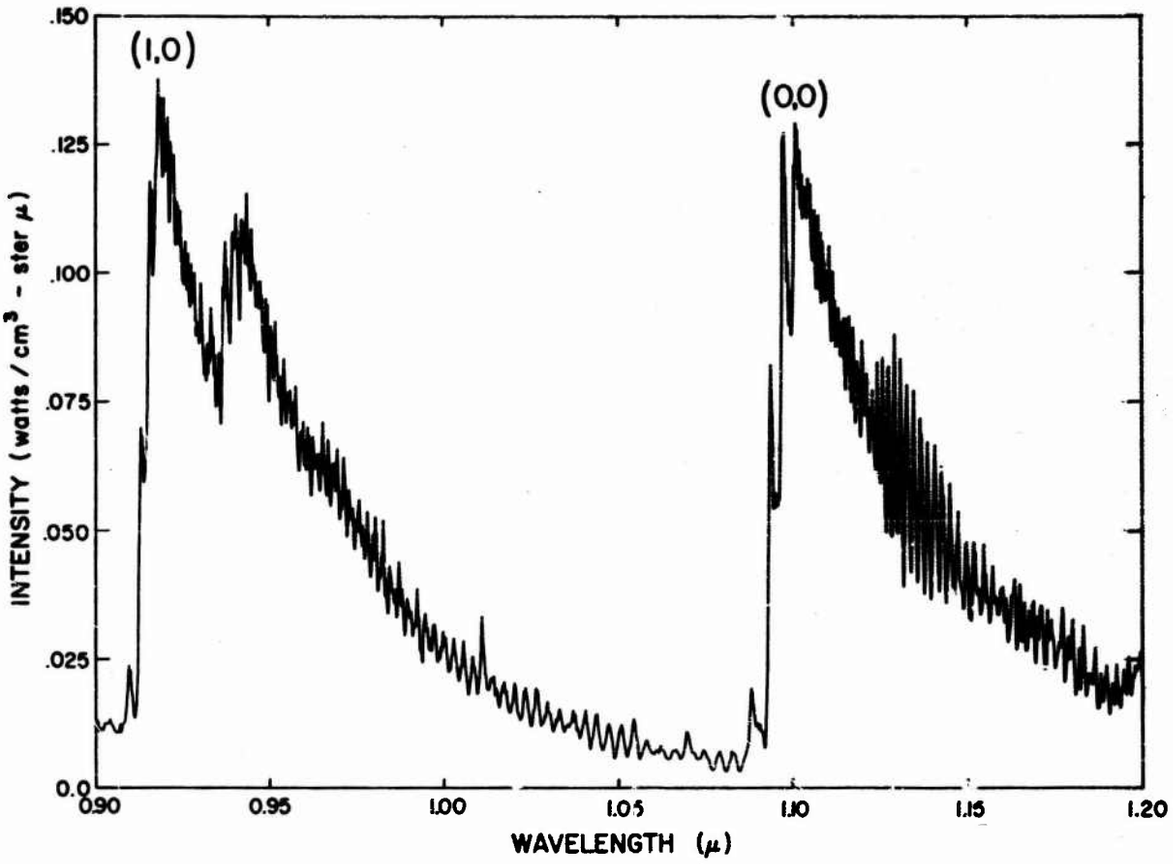

Fig. 7 CN red system spectrum obtained from arc heated nitrogen containing a "trace" of C_2H_6. Comparison with Fig. 6 shows that this system does not contribute significantly to the spectra under study.

IV. THEORETICAL MODEL

As indicated above, the radiation under investigation is undoubtedly due to nitric oxide. Radiation systems of NO have been investigated by many workers, including transitions involving the numerous Rydberg states, and the spectroscopic constants for the various states are available in the literature. A potential energy diagram has been prepared by Gilmore[17] and is reproduced in part in Fig. 8.

Using the relative energies of the v = 0 levels of the ten lowest Rydberg states (see Table I), the band origins were computed for all 45 conceivable transitions. These are given in Table II. As can be seen, of these 45 cases, 13 fall within the range of $0.8 \leq \lambda \leq 1.3\,\mu$. For one of these, $F^2\Delta \rightarrow D^2\Sigma^+$ (computed band origin at $\lambda = 1.142\,\mu$), $\Delta\Lambda = 2$ which is a forbidden transition for Hund's case b. $^2\Sigma^+$ states are always case b and the $F^2\Delta$ state is believed to be near case b.[26] Furthermore, electric discharge spectra[26] have never shown bands at the calculated position. Hence, this system was ruled out as an important contributor.

For the remaining 12 possible transitions, detailed spectral computations were carried out. In order to evaluate oscillator strengths from the experimental data the relative intensities of the radiation profiles for the transitions of interest were first calculated, i.e., the radiation intensities per NO particle (in units of watts/NO particle-ster-μ) were calculated as a function of wavelength, assuming that the product of the oscillator strength and the Franck-Condon factor equaled unity. These

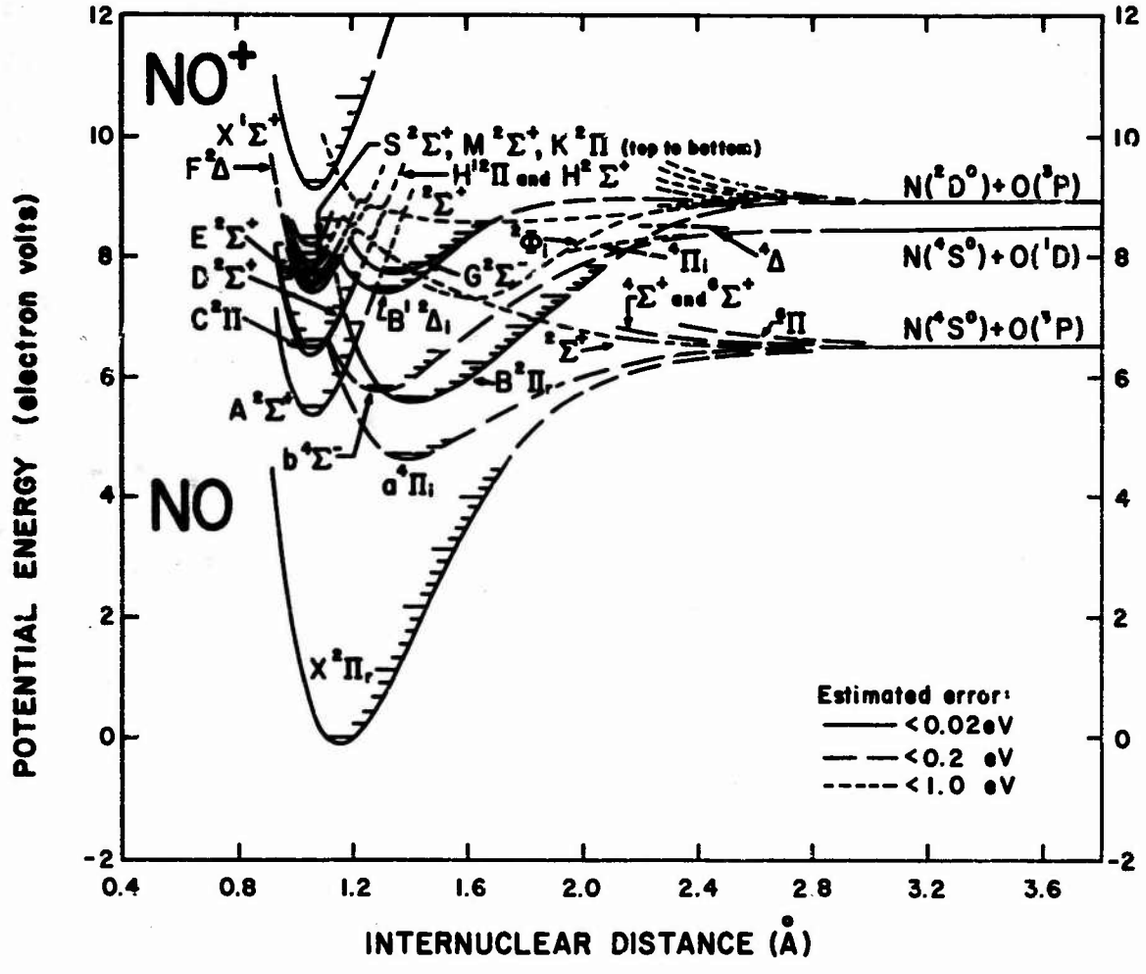

Fig. 8 Potential energy diagram for nitric oxide showing the various electronically excited states of interest in this study. From Ref. 17.

A7811

TABLE I

Relative Energies and Rotational Constants of the Ten Lowest Lying Rydberg States of Nitric Oxide

$T_0 (X^2\Pi_{\frac{1}{2}}) (v = 0) \equiv 0$

State	v	$T_0(cm^{-1})$	$B_v(cm^{-1})$	Refs.
$A^2\Sigma^+$	0	44199.2	1.9870	18
$A^2\Sigma^+$	1	46540.6	1.9688	18
$C^2\Pi$	0	52373	1.981	19, 20
$C^2\Pi$	1	54720	1.927	19, 20
$D^2\Sigma^+$	0	53291.2	1.9917	21
$D^2\Sigma^+$	1	55570.6	1.9701	21
$E^2\Sigma^+$	0	60862.8	1.9772	22, 23
$E^2\Sigma^+$	1	63204.7	1.9591	22, 23
$F^2\Delta$	0	62051.1	1.967	22
$F^2\Delta$	1	64367.7	1.852	22
$H^2\Sigma^+$	0	62705.5	1.994	24
$H^2\Sigma^+$	1	65044.9	1.976	24
$H'^2\Pi$	0	62717.3	2.006	24
$H'^2\Pi$	1	65056.4	1.985	24
$K^2\Pi$	0	64286	1.895	25
$K^2\Pi$	1	-	-	-
$M^2\Sigma^+$	0	64659	2.013	19, 25
$M^2\Sigma^+$	1	66972	1.995	19, 25
$S^2\Sigma^+$	0	67135	1.970	19, 25
$S^2\Sigma^+$	1	69480	1.950	25

TABLE II

Computed Band Origins for Transitions Between the Ten Lowest Lying Rydberg States of Nitric Oxide (Wavelength in Microns)

	$A^2\Sigma^+$	$C^2\Pi$	$D^2\Sigma^+$	$E^2\Sigma^+$	$F^2\Delta$	$H^2\Sigma^+$	$H'^2\Pi$	$K^2\Pi$	$M^2\Sigma^+$	$S^2\Sigma^+$
A	-	1.223	1.100	.6001	.5602	.5404	.5400	.4978	.4888	.4360
C		-	10.9	1.178	1.033	.9678	.9667	.8394	.8139	.6774
D			-	1.321	1.142	1.062	1.061	.9095	.8797	.7223
E				-	8.415	5.427	5.392	2.921	2.634	1.594
F					-	15.3	15.0	4.474	3.834	1.967
H						-	847.	6.327	5.119	2.258
H'							-	6.375	5.150	2.264
K								-	26.8	3.510
M									-	4.039
S										-

were computer calculations carried out for the Q, P and R branches of the 0, 0 and 1, 1 bands utilizing the Honl-London formulas[27] to get the relative line intensities and carrying rotational quantum numbers J up to 200. The lines were sorted according to wavelength and their intensities were summed in intervals of 13 Å, corresponding to the experimental resolution.

For Rydberg states the shape of the potential energy curves are almost indentical, the internuclear separation for the various states being very nearly equal (see Fig. 8). Hence, the Franck-Condon factors $q_{v'v''}$ are near unity for $\Delta v = 0$ and should be quite small for $\Delta v \neq 0$, as has indeed been theoretically computed for several NO Rydberg systems[28].

We give below the basic equations for carrying out this procedure. The equations are written from the point of view of absorption and all rotational quantum numbers J are understood to be for the absorbing state. The wave numbers $\nu(J)\ v'v''$ for each line (neglecting splitting) of the P, Q and R branches terminating in the J^{th} rotational level of the lower electronic state (vibrational level v'') are given by:

$$P: \quad \nu(J)(v'v'') = \nu_0(v'v'') + F_{v'}(J-1) - F_{v''}(J), \tag{1}$$

$$Q: \quad \nu(J)(v'v'') = \nu_0(v'v'') + F_{v'}(J) - F_{v''}(J), \tag{2}$$

$$R: \quad \nu(J)(v'v'') = \nu_0(v'v'') + F_{v'}(J+1) - F_{v''}(J), \tag{3}$$

where $\nu_0(v'v'')$ is the band origin. This is given by

$$\nu_0(v'v'') = T_0(v') - T_0(v''), \tag{4}$$

in which T_0 is the energy of the Rydberg state (J = 0) relative to the

ground state of NO ($X^2\Pi_{1/2}$) (see Table I). Furthermore, for all unperturbed states, the rotational energy is given by

$$F_v(J) = B_v J(J+1), \tag{5}$$

in which B_v is the rotational constant (see Table I).

The states $H^2\Sigma^+$ and $H'^2\Pi$ are very close energy wise (see Table I) and interact strongly.[24,29] The $H^2\Sigma^+$ state and the $^2\Pi_d$ component of the H' state are highly perturbed while the $^2\Pi_c$ component is uneffected. These effects can be summarized by the following:

$H'^2\Pi_c$: Eq. (5) is valid,

$$H'^2\Pi_d: \quad F_v(J) = B_v J(J+1) + 5.3\,J, \tag{6}$$

$$H^2\Sigma^+: \quad F_v(J) = B_v J(J+1) - 5.3\,J. \tag{7}$$

For the bands under study, which are very compact wavelength wise, the integrated absorption coefficient S(L) for each line is adequately given by[30]

$$S(L) = \frac{\pi e^2}{mc^2} f q_{v'v''} \frac{S_J}{\sum_{PQR} S_J} N, \tag{8}$$

where f is the absorption f-number or oscillator strength, and S_J is the rotational line strength or Honl-London factor.

N is the concentration of molecules in the absorbing state,

$$N = N_0 \frac{g''}{g_x} \frac{hcB_x}{kT} (2J+1) \left[1 - \exp(-hc\,\omega_x/kT)\right]$$
$$\exp\left\{-\left[T_0'' + v''\omega'' + F''(J)\right] hc/kT\right\}, \tag{9}$$

where N_0 is the total number of molecules (total number of nitric oxide molecules, regardless of quantum state), g is the electronic degeneracy, ω is the vibrational spacing and subscript x refers to the ground electronic state of NO; $\omega_x = 1890\ cm^{-1}$, $B_x = 1.705\ cm^{-1}$, [31] and

$$\omega'' = T_0''(v = 1) - T_0''(v = 0). \tag{10}$$

The literature values of T_0 and B_v for the v = 0 and v = 1 vibrational levels for the ten Rydberg states of interest are given in Table I. As discussed above, only the 0, 0 and 1, 1 bands were considered, i.e., in Eq. (8) we set $q(v' = v'') = 1$ and $q(v' \neq v'') = 0$ and considered only $v \leq 1$.

Finally, the spectral intensity per NO particle is given by

$$I = \frac{\bar{B} \sum_{\lambda'}^{\lambda' + \Delta\lambda} S(L)/N_0}{\Delta\lambda}\ ; \tag{11}$$

where $\bar{B}$ is the black body spectral intensity at the wavelength $(\lambda' + \Delta\lambda)/2$ and $\Delta\lambda = 13$ Å is the interval over which the individual lines are summed, which corresponds to the experimental resolution.

This procedure has been carried out at $T = 5700^{\circ}K$ for the 12 Rydberg transitions discussed above. The results of these calculations are shown in Figs. 9-14 where the intensity per NO particle is plotted on a logarithmic scale vs. wavelength for each transition. The P, Q and R branches are identified in the figures; band heads are noted by (h). For the two transitions involving the $H'^2\Pi$ state, the superscripts p and u are used on the branch identifications to indicate the perturbed and unperturbed substates, respectively.

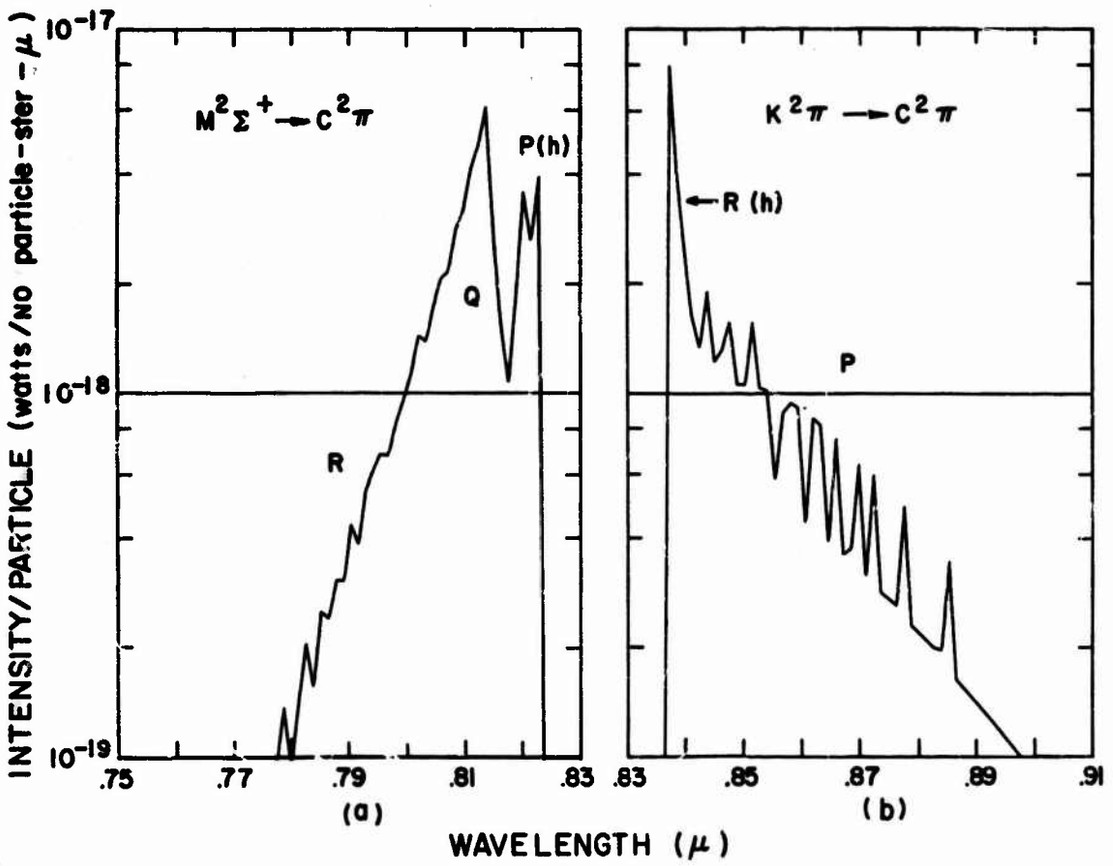

Fig. 9 Theoretically computed radiation intensity per particle as a function of wavelength for the nitric oxide Rydberg transitions (a) M → C and (b) K → C at T = 5700°K. The product of the Franck-Condon factor and the f-number was taken to be unity; in (a) the (0, 0) and (1, 1) bands are included, in (b) only the (0, 0) band was used.

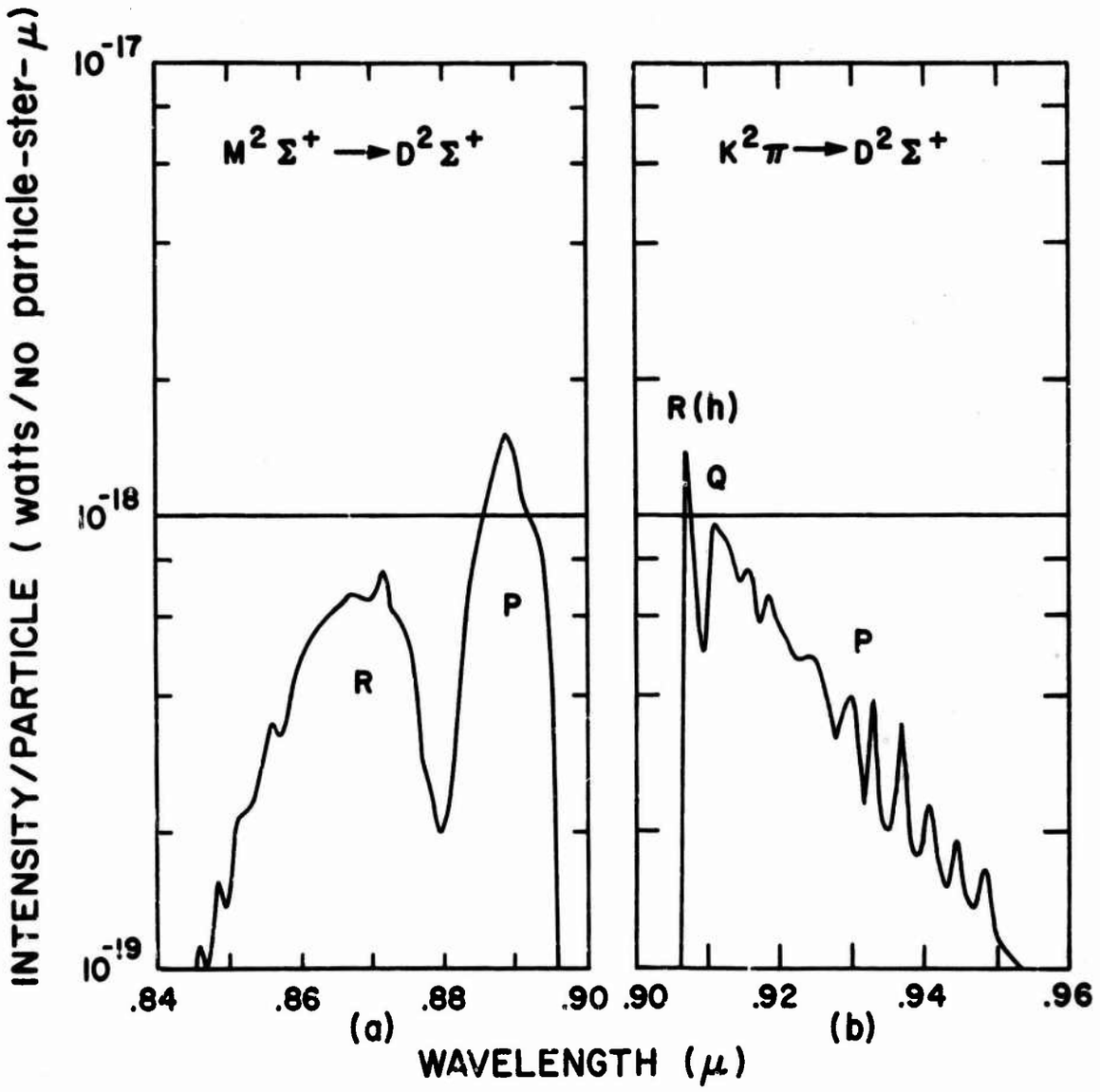

Fig. 10 Theoretically computed radiation intensity per particle as a function of wavelength for the nitric oxide Rydberg transitions (a) M → D and (b) K → D at T = 5700°K. The product of the Franck-Condon factor and the f-number was taken to be unity; in (a) the (0, 0) and (1, 1) bands are included, in (b) only the (0, 0) band was used.

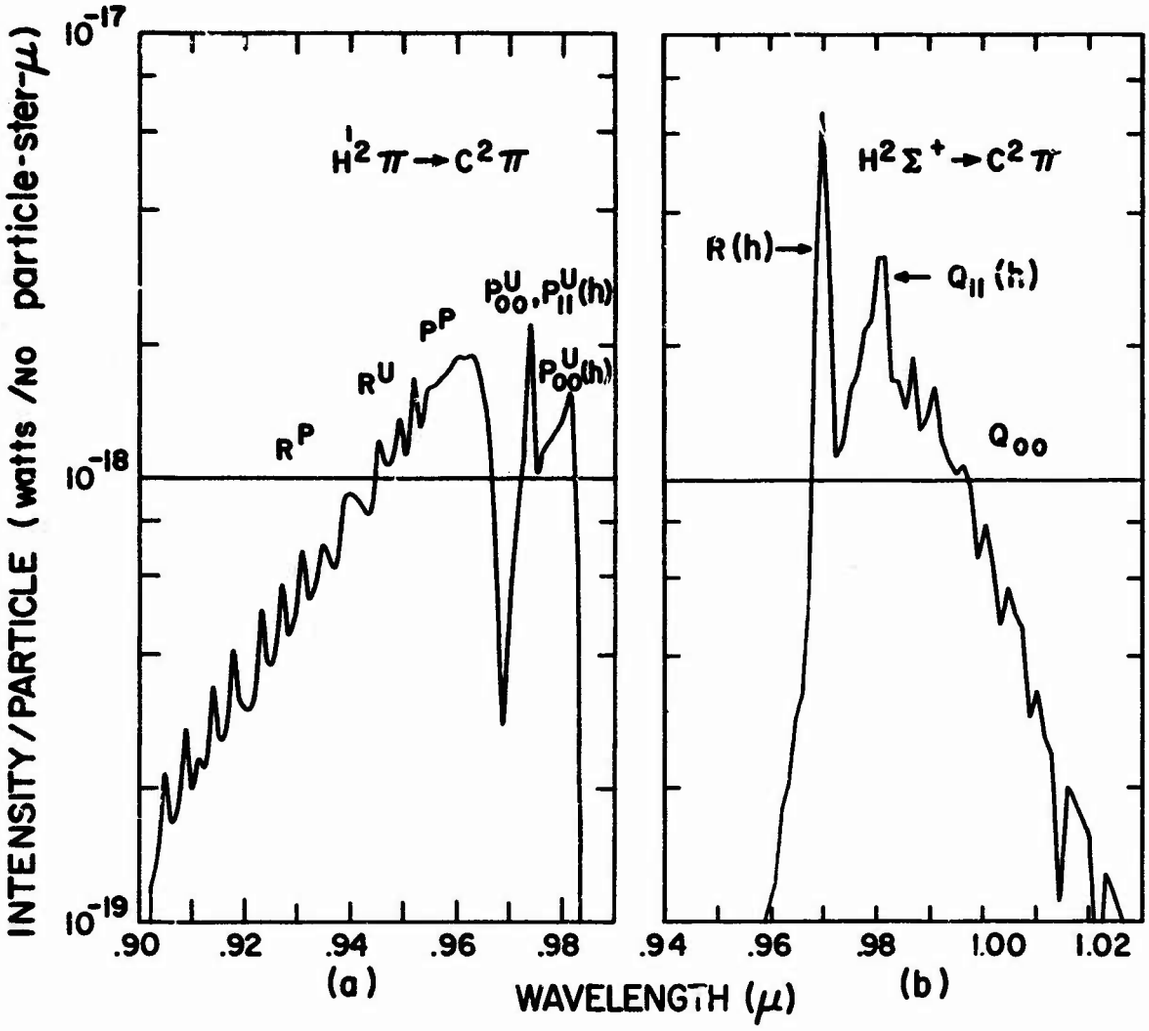

Fig. 11 Theoretically computed radiation intensity per particle as a function of wavelength for the nitric oxide Rydberg transitions (a) $H' \rightarrow C$ and (b) $H \rightarrow C$ at $T \approx 5700^{\circ}K$. The product of the Franck-Condon factor and the f-number was taken to be unity; only the (0, 0) and (1, 1) bands were included.

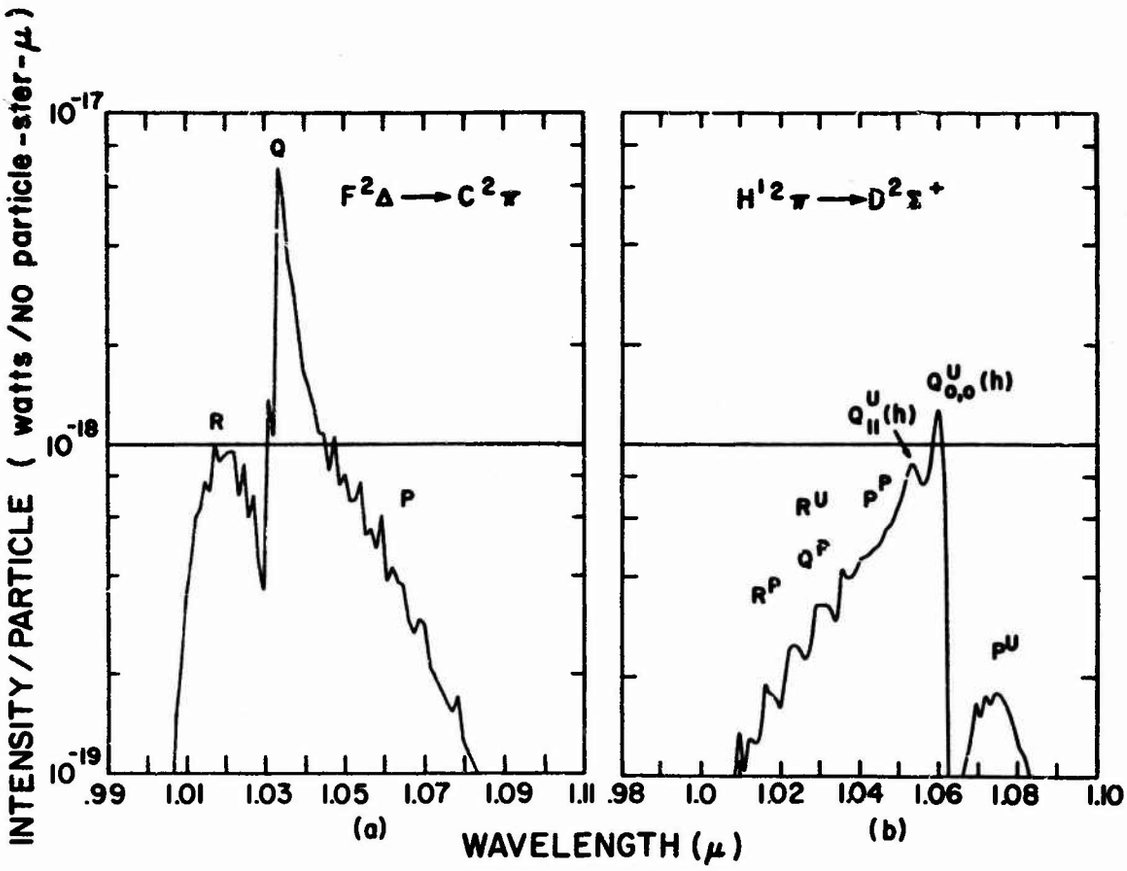

Fig. 12 Theoretically computed radiation intensity per particle as a function of wavelength for the nitric oxide Rydberg transitions (a) F → C and (b) H' → D at T = 5700°K. The product of the Franck-Condon factor and the f-number was taken to be unity; only the (0, 0) and (1, 1) bands were included.

A8388

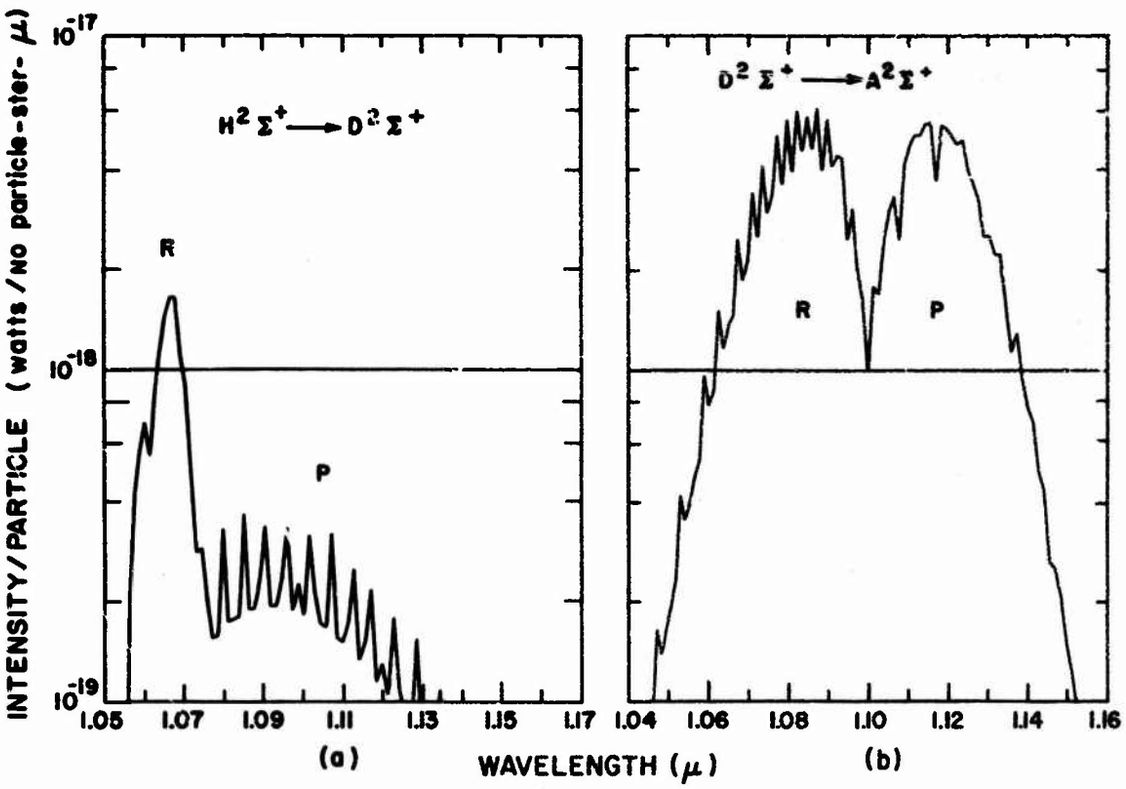

Fig. 13 Theoretically computed radiation intensity per particle as a function of wavelength for the nitric oxide Rydberg transitions (a) H → D and (b) D → A at T = 5700°K. The product of the Franck-Condon factor and the f-number was taken to be unity; only the (0, 0) and (1, 1) bands were included.

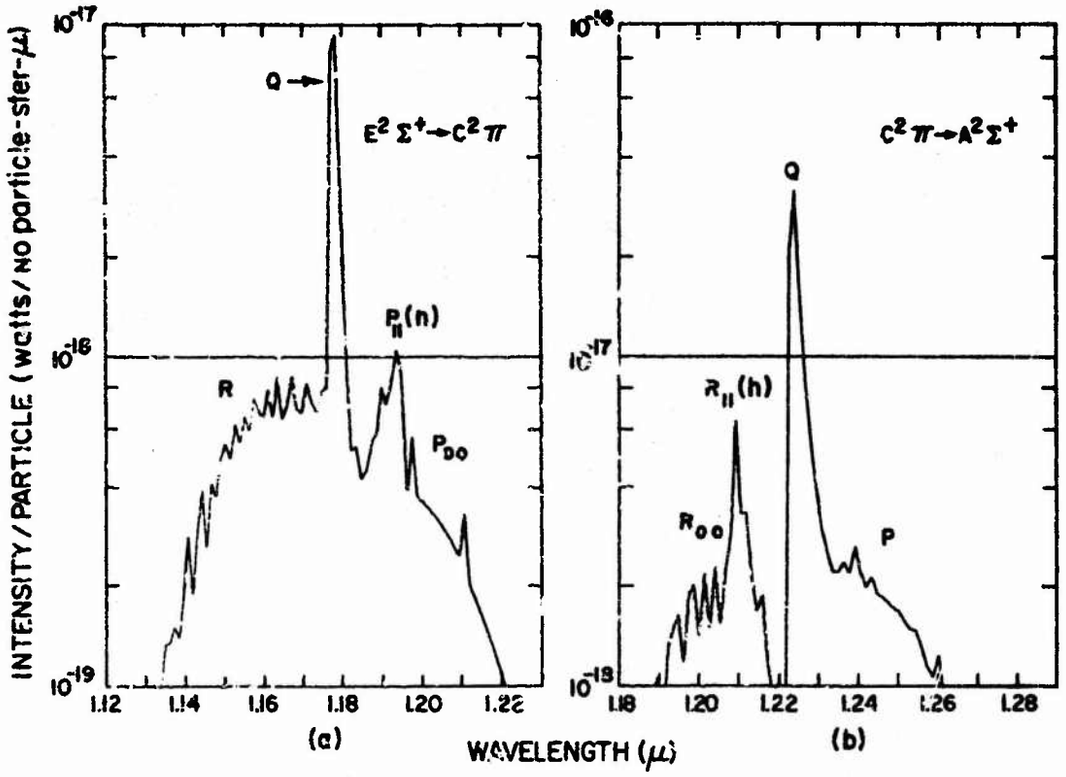

Fig. 14 Theoretically computed radiation intensity per particle as a function of wavelength for the nitric oxide Rydberg transitions (a) E → C and (b) C → A at T = 5700°K. The product of the Franck-Condon factor and the f-number was taken to be unity; only the (0, 0) and (1, 1) bands were included.

A8025

V. COMPARISON OF THEORY AND EXPERIMENT

Comparison of the theoretical spectra of Figs. 9-14 with the experimental spectra (Fig. 6) clearly shows many similar features. To make this comparison more qua titative and to properly take into account the wavelength overlap of the theoretical spectra in evaluating f-numbers, total synthetic spectra were computed.

Inspection of Figs. 9a, 9b and 10a shows that the M → C, K → C and M → D systems do not extend into the spectral region covered by the present experiment. No further comments regarding these three systems shall be made.

The K → D transition was not included in the synthetic spectrum since its wavelength distribution (Fig. 10b) showed a degradation to the red following the strong R-branch head at $\lambda = .9071\,\mu$. This obviously did not occur in the experimental spectra.

By comparing the experimental and theoretical curves for $T = 5700^{\circ}K$ at certain objectively chosen wavelengths, effective f-numbers for each of the remaining eight systems were estimated employing the number density of nitric oxide in air at 1 atm pressure and $5700^{\circ}K$ (see Table III). Since only vibrational levels v = 0 and 1 were considered in the theoretically calculated spectra shown in Fig. 9-14, a correction must be made for the contribution due to higher vibrational levels when these are used in conjunction with the experimental spectra to extract an f-number for each band system. Hence, in the total synthetic spectra we have multiplied each of the eight Rydberg intensities by the reciprocal of the fraction of

TABLE III

Equilibrium Concentrations in Particles per cc and Rydberg System Radiation Correction Factors to Account for Omission of States $v' \geq 2$

Species	Arc 5700°K	Arc 5800°K	Shock tube P_1 = 10 torr u_s = 3.44 mm/μsec 6300°K	Shock tube P_1 = 10 torr u_s = 3.58 mm/μsec 6550°K
NO	1.34×10^{16}	1.22×10^{16}	7.0×10^{17}	6.2×10^{17}
N_2	7.23×10^{17}	6.91×10^{17}	1.3×10^{19}	1.2×10^{19}
O_2	5.90×10^{14}	4.75×10^{14}	5.8×10^{16}	4.7×10^{16}
N	1.36×10^{17}	1.57×10^{17}	1.6×10^{18}	2.2×10^{18}
O	4.13×10^{17}	4.03×10^{17}	6.9×10^{18}	7.0×10^{18}
e	1.83×10^{14}	2.08×10^{14}	3.5×10^{15}	4.9×10^{15}
$\frac{NO^*(\text{all } v)}{NO^*(v=0,1)}$	1.48	1.50	1.57	1.60

molecules in the v = 0 and 1 levels. This has the effect of properly satisfying the statistical mechanics but it forces the radiation from the $v' > 2$ states to have the same wavelength dependence as does the $v' = 0$ and 1. This is undoubtedly incorrect in detail but is the best that can be presently done. This correction factor was calculated to be 1.48 at T = 5700 and 1.50 at T = 5800°K.

In addition to the eight Rydberg transitions, the synthetic spectrum also included contributions from the $N_2(1+)$ system and neutral Bremsstrahlung. The $N_2(1+)$ radiation was computed using the smeared rotational model and f-number[6] of 3.38×10^{-3}.

The neutral Bremsstrahlung radiation intensity was computed from the equation[32]

$$I = \frac{16\pi e^6}{3\sqrt{3}\, mc^2} \frac{e^{-hc/kT\lambda}}{\lambda^2 (2\pi mkT)^{1/2}} [n_e] \sum_i Z_i^2 [n_i], \qquad (12)$$

where e and m are the charge and mass, respectively, of the electron, $[n_e]$ is the concentration of electrons, Z_i is the "effective coulombic charge" of the neutral species $[n_i]$ doing the scattering, and the summation is over all species. The effective Z^2 for relevant species was obtained by extrapolating the recent work of Taylor[32] to 1μ; this yielded $Z^2_{N_2} = 3.2 \times 10^{-2}$, $Z^2_N = 3.0 \times 10^{-2}$, and $Z^2_O = 2.0 \times 10^{-2}$. The species concentration are given in Table III for conditions of interest.

Using the estimated NO oscillator strengths, and the appropriate number densities, a theoretical synthetic spectrum was computed at

$T = 5700^{\circ}K$ by summing over the eight Rydberg band systems plus the $N_2(1+)$ band system and the neutral Bremsstrahlung. This synthetic spectrum was compared to the experimental spectrum and adjustments were made in the NO f-numbers to ultimately make the best subjective fit to the entire spectrum. The NO Rydberg f-numbers finally arrived at are given in Table IV. The final theoretical synthetic spectrum calculation is shown in Fig. 15 along with the experimental data obtained at $5690^{\circ}K$. In the theoretical plot the eight Rydberg and the $N_2(1+)$ contributions are shown along with the upper curve which is the sum of all the contributions.

In Fig. 16 the sum curve of the synthetic spectrum at $T = 5800^{\circ}K$ is compared to the experimental curve at the same temperature. This experimental spectrum represents the best data at $\lambda > 1.05\,\mu$, but no readjustments of the oscillator strengths were made because of it.

As can be seen in the synthetic spectra, the $N_2(1+)$ radiation makes an important contribution, especially in the vicinity of the 0, 0 band head. On the other hand, the neutral Bremsstrahlung is negligible for the conditions of Figs. 15 and 16; over the wavelength interval $0.9 - 1.2\,\mu$ the Bremsstrahlung intensity is essentially constant and at $5700^{\circ}K$, equal to 1.1×10^{-3} watts/cc-ster-μ.

It should be pointed out that the starting wavelengths for the 13 Å intervals over which the rotational lines were summed were arbitrarily located when the calculations shown in Figs. 9-14 were carried out. By changing these starting wavelengths slight differences in the synthetic spectra resulted but were of no significant importance. In constructing

TABLE IV

Experimentally Determined Oscillator Strengths for Transitions Between Rydberg States of Nitric Oxide in the Wavelength Region 0.9 to 1.2 microns

Transition	Oscillator Strength
$K^2\Pi \rightarrow D^2\Sigma^+$	< .08
$H'^2\Pi \rightarrow C^2\Pi$	.15
$H^2\Sigma^+ \rightarrow C^2\Pi$	.12
$F^2\Delta \rightarrow C^2\Pi$	.22
$H'^2\Pi \rightarrow D^2\Sigma^+$	.50
$H^2\Sigma^+ \rightarrow D^2\Sigma^+$	.25 (>.07)
$D^2\Sigma^+ \rightarrow A^2\Sigma^+$	.18
$E^2\Sigma^+ \rightarrow C^2\Pi$	< .03
$C^2\Pi \rightarrow A^2\Sigma^+$	.70

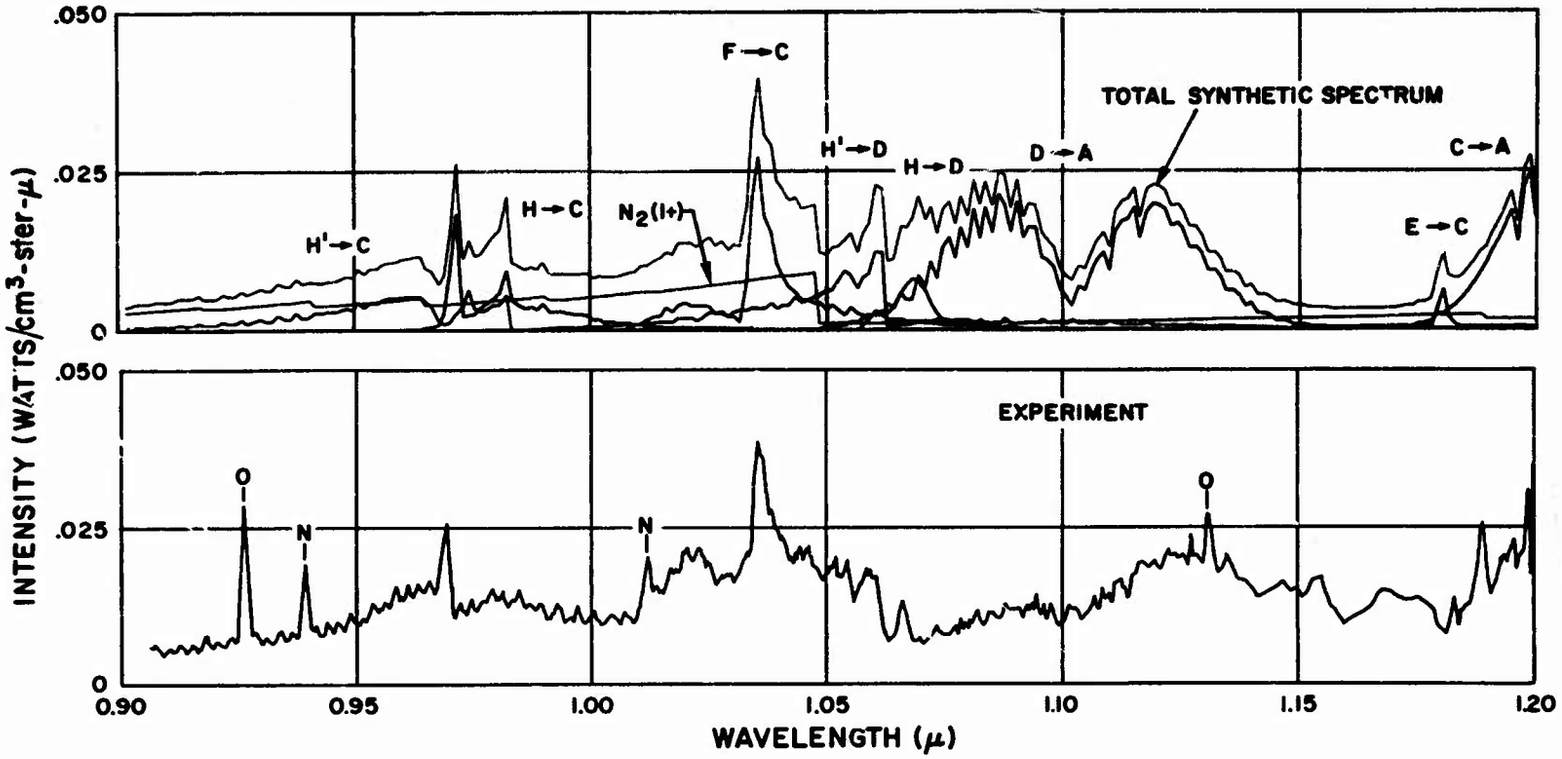

Fig. 15 Comparison of the theoretically computed spectral intensity from air at T = 5700°K with the experimental results. The experimental curve is the same as that shown in Fig. 6 (T = 5690°K). The top theoretical curve represents the sum of the contributions from eight NO Rydberg transitions and the N_2 (1+) system. The NO f-numbers used are tabulated in Table IV.

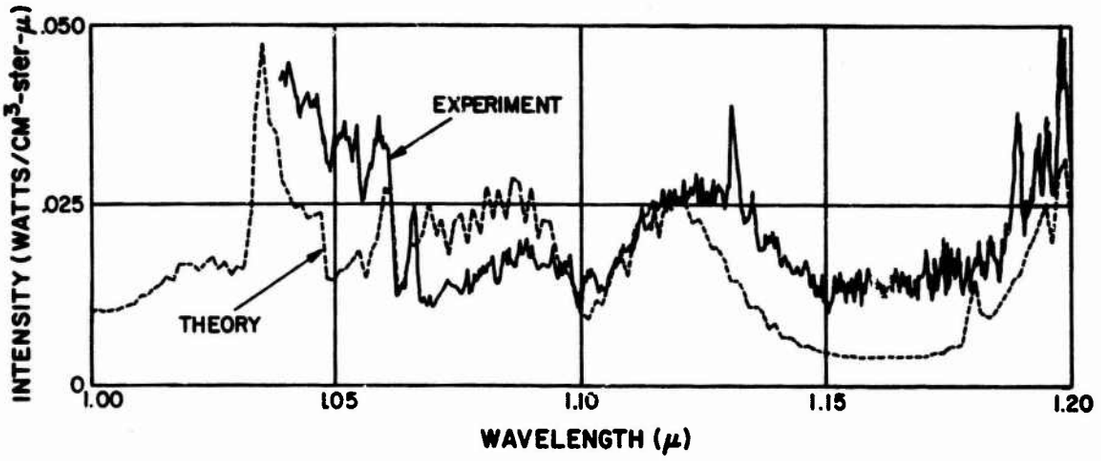

Fig. 16 Comparison of the theoretically computed spectral intensity from air at T = 5800°K with the experimental results. The experimental curve is the same as that shown in Fig. 6 (T = 5800°K) and is the most accurate at $\lambda > 1.05\,\mu$. The f-numbers used are tabulated in Table IV.

the total synthetic spectra shown in Fig. 15, the starting wavelength was not the same as the individual cases (Figs. 9-14) and hence minor differences may be found.

The transition $E^2\Sigma^+ \rightarrow C^2\Pi$ was included in the calculations with an assigned f-number of 0.03, this value being finally chosen so as to make the presence of this system just recognizable in the synthetic spectrum. However, as is seen in Figs. 15 and 16, it is not discernable in the experimental spectra. On this basis an upper bound of $f < 0.03$ is set for the $E \rightarrow C$ transition. This is in agreement with the fact that this system has not been observed in electric discharge spectra[33].

As was stated above, the $K^2\Pi \rightarrow D^2\Sigma^+$ was not included in the synthetic spectrum due to its obvious unimportance. However, an upper bound of $f < .08$ was determined for this system by assigning the R-branch head a maximum intensity of 1.5×10^{-3} watts/cc-ster-μ.

As was described in Section III, an O-line and two N-lines were used to establish the wavelength scale of the experimental spectra. Furthermore, subsequent to data reduction, another O-line ($\lambda \approx 1.130\mu$) was clearly identified. It is of some value to compare the experimental intensities of these lines with theoretical calculated intensities.

For the optical thin case, the line intensity per unit volume per steradian is given by

$$I = \frac{2\pi he^2}{m\lambda^3} \frac{g''}{g'} f N^* , \qquad (13)$$

where f is the absorption f-number of the line, g'' and g' are the degeneracies of the lower and upper electronic states involved in the

transition and N^* is the concentration of the radiating state. The spectroscopic parameters necessary to carry out this calculation for the O and N lines of interest are given by Griem,[34] including theoretical values for f.

The experimental values for the line intensities were obtained from the 5690°K spectrum by subtracting the background band intensity from the peak line intensity and multiplying the remainder by the experimental resolution (13 Å).

The theoretical and experimental line intensities at 5690°K are compared in Table V. The second column of this table gives the range of wavelengths for each group of multiplets, e.g., the first O-line actually is composed of 9 lines with a total degeneracy of 60.

Included in Table V are two additional N-lines at 1.0506 and 1.0539-1.0548μ. It is not clear that these lines are seen experimentally. They are included in the table because within the spectral range of the present experiment, they would be theoretically the next most intense lines following the other 4 lines in the table which have been positively identified in the experimental spectra.

The last column in Table V gives the ratio of the experimental to calculated line intensities. For the 4 lines which are positively identified in the spectra, this ratio varied between 1.5 and 4.2. Although some of this disagreement might be assigned to the theoretical f-numbers being too small, probably most of it is due to fluctuation in the arc temperature. For these lines, the radiating states are at approximately 12 eV (see third column, Table V) and, hence, temperature fluctuations of the order of

TABLE V

Comparison of Theoretical and Experimental Atomic Line Intensities at T = 5690°K. (Intensities in watts/cc-ster)

Atom	λ_{lit}	E(ev)	I_{calc}	I_{exp}	I_{exp}/I_{calc}
O	.9261-66	12.03	1.88×10^{-5}	2.8×10^{-5}	1.5
N	.9387-93	11.96	3.64×10^{-6}	1.4×10^{-5}	3.8
N	1.0113	12.93	1.69×10^{-6}	7.1×10^{-6}	4.2
N	1.0506	12.96	1.88×10^{-7}	$< 30 \times 10^{-7}$	< 16
N	1.0539-48	12.96	4.36×10^{-7}	$< 30 \times 10^{-7}$	< 7
O	1.1295-302	11.79	2.90×10^{-6}	1.1×10^{-5}	3.8

several hundred degrees can account for the high experimental values of the line intensities.

Although in the present experimental work the spectral scans went only to 1.20μ, it is felt that the shoulder of the R-branch of the $C^2\Pi \rightarrow A^2\Sigma$ system is clearly observed in the spectra. The most prominent portion of this system is the extremely strong Q branch at 1.224μ (see Fig. 14 b). This is, in all probability, the source of the strong radiation at 1.22μ reported by Wurster, et al,[2,7] which radiation was attributed by them to an unidentified atomic line. Employing the species concentrations (see Table III) appropriate to the reflected shock conditions corresponding to $T = 6300^{\circ}K$ (Ref. 2) and $T = 6550^{\circ}K$ (Ref. 7), synthetic spectra were calculated and are shown along with the data of Wurster, et al in Fig. 17. Their spectral resolution was 80 Å. For these cases, atomic line radiation is negligible.

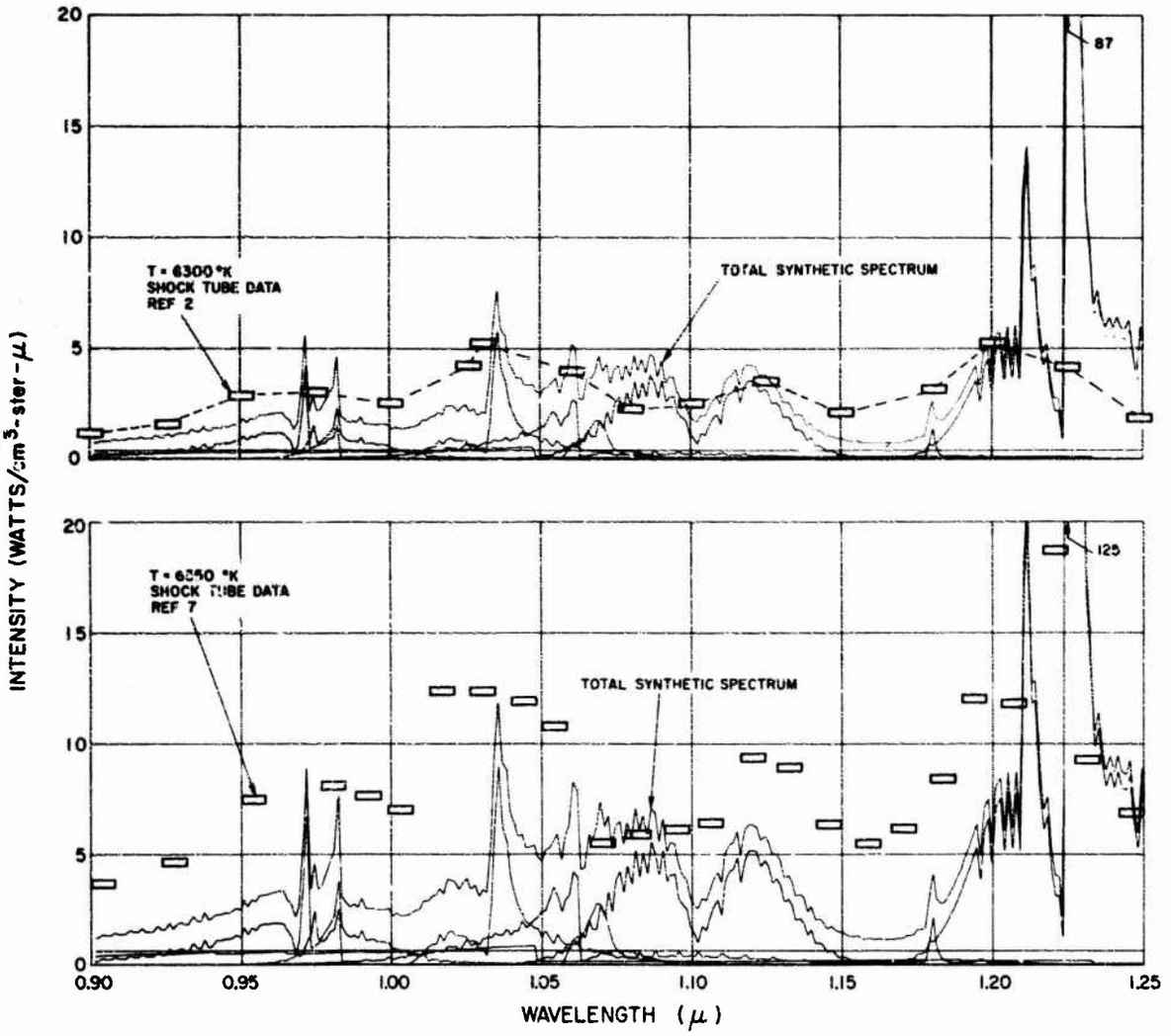

Fig. 17 Comparison of the theoretically computed spectral intensity from air at T = 6300°K (top spectrum) and 6500°K (bottom spectrum) with the shock tube data of Wurster, et al.[2,7] The total synthetic spectral curves are the sum of the contributions from eight NO Rydberg transitions, the N_2 (1+) system and the neutral Bremsstrahlung. The NO f-numbers used are tabulated in Table IV.

VI. DISCUSSION

Fig. 15 shows that the synthetic spectrum resembles the experimental one in considerable detail, even more so when the atomic lines are accounted for. However, there do exist several apparent anomalies which are discussed below.

In the experimental spectra a rather sharp radiation peak appears at $\lambda = 1.0661\mu$; its counterpart in the synthetic spectrum is about three times as wide and is due to the R-branch of the H → D transition. However, here it is known that the model is inadequate. According to Huber[29] the R-branch in the H → D (0, 0) system is strongly perturbed for $J > 29$, producing a head at $\lambda = 1.0657\mu$. This perturbation is ascribed to the H state. Because of this effect, the oscillator strength for the $H^2\Sigma^+ \rightarrow D^2\Sigma^+$ system could be as small as 1/3 the value of .25 used in computing the final synthetic spectrum, as is noted in Table IV.

The most apparent anomaly is the presence of a radiation spike at $\lambda = .9810\mu$ in the synthetic spectrum which is absent in the experimental spectrum. This radiation peak is produced in the synthetic spectrum by equal contributions from the H' → C and H → C systems. In the former case, this radiation is due to a head formation at J = 81 in the Pu branch of the 0, 0 transition only. In the latter case the Q branch of the 1, 1 transition forms a head at J = 54. Clearly, the presence of this anomaly is due to an inadequate model. Perturbation at high J values might not even allow these heads to form. In any event, note that in both cases only one of the two vibrational transitions included in the model

contributed. Hence, the inherent error in the correction factor for $v' \geq 2$ discussed above is clearly pointed out here.

Inspection of Figs. 15, 16 and 17 shows that for both the arc and shock tube cases, the synthetic spectra predict too little radiation in the region 1.15 - 1.17μ. The experimental spectra lack distinguishing features at this wavelength and the source of this radiation is uncertain.

Although the agreement between experimental and synthetic spectra in the vicinity of the D → A transition is not perfect, it is considered satisfactory. The distinct R and P branches are clearly seen in the experimental spectra of Fig. 6 - perhaps more readily in the spectra other than the one reproduced in Fig. 15. Although the theoretical spectrum (Fig. 13b) shows a symmetrical R and P branch, the experimental R branch maximum is somewhat less than the P branch maximum.

Since the oscillator strengths for these Rydberg transitions are quite high, the question arises as to whether the radiation approaches the black body limit at any wavelength in the present experiment. The most likely wavelength for this to occur would be at $\lambda = 1.224\mu$, the peak of the Q branch of the $C^2\Pi \rightarrow A^2\Sigma$ transition. For this case, at 5700°K, it is found that the J = 31 and J = 32 lines (which produce the maximum intensity) are 0.55 Å apart while the doppler width is 0.12 Å; thus the lines do not overlap. The intensity of the J = 32 line is 4.9×10^{-5} watts/cm^2-ster or 4.1 watts/cm^2-ster-μ at the line center; this is to be compared to 6.7×10^2 watts/cm^2-ster-μ for black body radiation at the same wavelength and temperature. Thus the line is not black and blackness cannot be considered a source of error in the present experiment.

A similar analysis for the reflected shock wave conditions of Fig. 17 shows that the line centers definitely are black. This probably accounts for the substantial quantitative difference between Wurster's data[2,7] and the synthetic spectrum in the vicinity of the Q branch peak of the C → A transition. No attempt was made to correct the calculations for blackness. Otherwise, the agreement between the synthetic spectra and the shock tube data is considered satisfactory.

There are three known NO band systems which radiate in the wavelength region of interest which have not been included in the synthetic spectra. The non-Rydberg system $B'^2\Delta \rightarrow B^2\Pi$ has its 0, 0 band at $\lambda = .6872\mu$[35] and the bands degrade to the violet. From the equation given in Ref. 35 we calculate that the 0, 4 band is at $\lambda = .9478\mu$; Nicholls[28] gives $q_{0,4} = 7.0 \times 10^{-2}$. With $T_0 = 7.45$ e v for the $B'^2\Delta$ state, it is highly unlikely that this transition contributes significantly in the present study. From an equation similar to that of Eq. (13), but including the Frank-Condon factor, it is found that at 5700°K, $I = 6 \times 10^{-4} \frac{f}{\Delta\lambda}$ watts/cc-ster-μ, where $\Delta\lambda$ is the wavelength extent of the 0, 4 band in microns. If 1×10^{-2} watts/cc-ster-μ is taken as the intensity level necessary to dominate the experimental spectrum, and $\Delta\lambda \approx 5 \times 10^{-2}\mu$, then $f \approx 0.9$. For a non-Rydberg system, the expected f-number would be much smaller than that. The absence of a prominent spectral feature near $.95\mu$ also indicates that this system is negligible in the present study.

The Ogawa system $b^4\Sigma^- \rightarrow a^4\Pi$ also radiates in the spectral region of interest. The 0, 0 band shows six strong heads from .9617

to .9732μ and the band degrades to the violet[36]. By a similar calculation as that done above (T_0 = 5.80 ev, $q_{0,0}$ = .25[28]), we find that $f \approx 4 \times 10^{-3}$ for this system to be important at 5700°K. The absence of the six headed band in the experimental data would seem to rule out the significance of this system in the present work, although it may be making a small contribution to the experimental intensity.

Finally, the non-Rydberg → Rydberg transition $B'^2\Delta \rightarrow C^2\Pi$ (4, 1) should be considered. This system, which is discussed in detail in Ref. 29, is caused by perturbations in B'(v = 4) by $F^2\Delta$ (v=1) and in C(v = 1) by $B^2\Pi$ (v = 10). The lines of the strong Q branch of this transition accumulate at λ = 1.025μ. This system could be making a finite but not overwhelming contribution in this wavelength region. However, it is not possible to clearly evaluate this with the present data.

It is very difficult in an experiment such as this to evaluate in a rigorous quantitative manner the possible errors associated with the oscillator strengths given in Table IV. Comparisons of the absolute value of the intensities of several high temperature (T ≈ 5700 - 5800°K) experimental spectra such as the ones treated quantitatively above, indicate reproducibility to about 30%. For the transitions involved, the T_0 values are sufficiently small so that arc temperature fluctuations of the order of several hundred degrees produce uncertainties of about this value. Because of the overlap of the various spectra, uncertainties in the f-number of the $N_2(1+)$ system and the questionable treatment of states $v' \geq 2$, it is estimated that the f-numbers given in Table IV are correct to within a factor of two.

The present investigation has employed a 1 atm constricted arc to study the radiation emanating from hot air in the 1μ region; high resolution spectra were taken. A comparison of these spectra with spectra taken of discharges in various gases has shown that the source of the "excess air radiation" requires the presence of both nitrogen and oxygen nuclei. Comparison of the high resolution equilibrium air spectra with calculated synthetic spectra arising from the Rydberg states of nitric oxide showed good correlation of most of the spectral features. The oscillator strengths for nine NO-Rydberg systems have been evaluated in the wavelength range of 0.9 - 1.2μ.

VII. ACKNOWLEDGMENTS

The author wishes to acknowledge the aid given by Messrs. H. Koritz and E. Feldman in running the arc facility and reducing data and P. MacLean in carrying out the many computer calculations of the theoretical spectrum.

REFERENCES

1. T. Wentink, W. Planet, P. Hammerling and B. Kivel, J. Appl. Phys. 29, 742 (1958).
2. W. H. Wurster, C. E. Treanor and H. M. Thompson, J. Chem. Phys. 37, 2560 (1962).
3. J. C. Keck, J. Camm, B. Kivel and T. Wentink, Ann. Phys. 7, 1 (1959).
4. W. H. Wurster, J. Chem. Phys. 36, 2111 (1962).
5. R. A. Allen, J. C. Camm and J. C. Keck, JQSRT 1, 269 (1961).
6. K. L. Wray and T. J. Connolly, JQSRT 5, 111 (1965).
7. W. H. Wurster and P. V. Marrone, JQSRT 7, 591 (1967).
8. J. C. Keck, R. A. Allen and R. L. Taylor, JQSRT 3, 335 (1963).
9. K. L. Wray, P. H. Rose and H. E. Koritz, Avco Everett Research Laboratory Research Report 226 (August 1965).
10. K. L. Wray and N. H. Kemp, AIAA 3rd Aerospace Sciences Meeting, January 24-26, 1966, New York, AIAA Paper No. 66-56.
11. K. L. Wray, unpublished data, June 1965.
12. D. L. Ford and J. H. Shaw, Appl. Optics 4, 1113 (1965).
13. R. M. Feinberg and M. Camac, JQSRT 7, 581 (1967).
14. E. Miescher, JQSRT 2, 421 (1962).
15. W. H. Wurster and P. V. Marrone, Annual Report QM-1373-A-4, (Cornell Aeronautical Laboratory) July 1960-June 1961 (July 1961).
16. R. E. B. Pearse and A. G. Gaydon, "The Identification of Molecular Spectra", 3rd Ed. London: Chapman & Hull Ltd (1963).

17. F. R. Gilmore, Rand Memo RM-4034-PR (June 1964).

18. L. Gero and R. Schmid, Proc. Phys. Soc. 60, 533 (1948).

19. E. Miescher, JQSRT 2, 421 (1962).

20. G. Herzberg, A. Lagerqvist and E. Miescher, Can. J. Phys. 34, 622 (1956).

21. R. F. Barrow and E. Miescher, Proc. Phys. Soc. 70A, 219 (1957).

22. K. Dressler and E. Miescher, Astrophys. J. 141, 1266 (1965).

23. M. W. Feast, Can. J. Phys. A28, 488 (1950).

24. K. P. Huber and E. Miescher, Helv. Phys. Acta 36, 257 (1963).

25. A. Lagerqvist and E. Miescher, Can. J. Phys. 44, 1525 (1966).

26. A. Lagerqvist and E. Miescher, Can. J. Phys., 40, 352 (1962).

27. G. Herzberg, "Spectra of Diatomic Molecules", 2nd Ed. New York: Van Nostrand 1950, p 208.

28. R. W. Nicholls, J. of Research of the National Bureau of Standards, A. Physics and Chemistry 68A, 535 (1964).

29. M. Huber, Helv. Phys. Acta. 37, 329 (1964).

30. A. Schadee, JQSRT 7, 169 (1967).

31. G. Herzberg, op. cit., p 558.

32. R. Taylor and G. Caledonia, Experimental Determination of the Cross Section for Neutral Bremsstrahlung II. High Temperature Air Species - O, N, and N_2. To be published.

33. M. W. Feast, Can. J. of Res. A28, 488 (1950).

34. H. Griem, "Plasma Spectroscopy". New York: McGraw-Hill 1964.

35. M. Ogawa, Science of Light 2, 87 (1953).

36. M. Brook and J. Kaplan, Phys. Rev. 96, 1540 (1954).

UNCLASSIFIED

Security Classification

DOCUMENT CONTROL DATA - R&D

(Security classification of title, body of abstract and indexing annotation must be entered when the overall report is classified)

1 ORIGINATING ACTIVITY (Corporate author) Avco Everett Research Laboratory 2385 Revere Beach Parkway Everett, Massachusetts	2a REPORT SECURITY CLASSIFICATION Unclassified 2b GROUP

3 REPORT TITLE

Oscillator Strengths of Transitions between Rydberg States of Nitric Oxide in the Near IR

4 DESCRIPTIVE NOTES (Type of report and inclusive dates)

Research Report 300

5 AUTHOR(S) (Last name, first name, initial)

Wray, Kurt L.

6 REPORT DATE	7a TOTAL NO. OF PAGES	7b NO. OF REFS
February 1969	54	36

8a CONTRACT OR GRANT NO. F04701-68-C-0036 b PROJECT NO. c d	9a ORIGINATOR'S REPORT NUMBER(S) Research Report 300 9b OTHER REPORT NO(S) (Any other numbers that may be assigned this report) SAMSO-TR-69-29

10 AVAILABILITY/LIMITATION NOTICES

This document has been approved for public release and sale. Its distribution is unlimited.

11 SUPPLEMENTARY NOTES	12 SPONSORING MILITARY ACTIVITY Advanced Research Projects Agency, Department of Defense, ARPA Order #1092 and Space and Missile Systems Organization, Air Force Systems Command, Deputy for Re-entry Systems (SMY), Norton Air Force Base, California 92409.

13 ABSTRACT

In recent years several shock tube studies have been made of the radiation emanating from hot air and nitrogen in the near IR. These investigations showed about 10 times more radiation from air than could be accounted for on the basis of the $N_2(1+)$ band systems alone; however, there has been some controversy as to the source of this excess air radiation. The present experiments utilized a continuously running 1 atm constricted arc jet to prepare equilibrium air and nitrogen at temperatures between 3500 and 5800°K. The excess air radiation was confirmed, and it was shown that it requires the presence of both N and O nuclei. High resolution spectra (13 Å) were obtained from .9 to 1.2 μ employing a scanning monochromator and photomultiplier. Most of the features of these air spectra could be correlated with transitions arising between Rydberg states of NO. Employing the available spectroscopic parameters, theoretical calculations of the wavelength dependence of the radiation were made. By comparing the calculated total synthetic spectra with the experimental spectra, f-numbers for nine NO Rydberg systems have been evaluated.

DD FORM 1 JAN 64 1473

UNCLASSIFIED

Security Classification

UNCLASSIFIED

Security Classification

KEY WORDS	LINK A		LINK B		LINK C	
	ROLE	WT	ROLE	WT	ROLE	WT
1. Nitric oxide radiation						
2. Rydberg states of NO						
3. Oscillator strengths						
4. Near IR radiation						
5. Arc heated air						
6. Air IR radiation						
7. N_2 (1+) Radiation						

INSTRUCTIONS

1. ORIGINATING ACTIVITY: Enter the name and address of the contractor, subcontractor, grantee, Department of Defenae activity or other organization *(corporate author)* issuing the report.

2a. REPORT SECURITY CLASSIFICATION: Enter the overall security classification of the report. Indicate whether "Restricted Data" is included. Marking is to be in accordance with appropriate security regulations.

2b. GROUP: Automatic downgrading is specified in DoD Directive 5200.10 and Armed Forces Industrial Manual. Enter the group number. Also, when applicable, show that optional markings have been used for Group 3 and Group 4 as authorized.

3. REPORT TITLE: Enter the complete report title in all capital letters. Titles in all cases should be unclassified. If a meaningful title cannot be selected without classification, show title classification in all capitals in parenthesis immediately following the title.

4. DESCRIPTIVE NOTES: If appropriate, enter the type of report, e.g., interim, progress, summary, annual, or final. Give the inclusive dates when a specific reporting period is covered.

5. AUTHOR(S): Enter the name(s) of author(s) as shown on or in the report. Enter last name, first name, middle initial. If military, show rank and branch of service. The name of the principal author is an absolute minimum requirement.

6. REPORT DATE: Enter the date of the report as day, month, year, or month, year. If more than one date appears on the report, use date of publication.

7a. TOTAL NUMBER OF PAGES: The total page count should follow normal pagination procedures, i.e., enter the number of pages containing information.

7b. NUMBER OF REFERENCES: Enter the total number of references cited in the report.

8a. CONTRACT OR GRANT NUMBER: If appropriate, enter the applicable number of the contract or grant under which the report was written.

8b, 8c, & 8d. PROJECT NUMBER: Enter the appropriate military department identification, such as project number, subproject number, system numbers, task number, etc.

9a. ORIGINATOR'S REPORT NUMBER(S): Enter the official report number by which the document will be identified and controlled by the originating activity. This number must be unique to this report.

9b. OTHER REPORT NUMBER(S): If the report has been assigned any other report numbers *(either by the originator or by the sponsor)*, also enter this number(s).

10. AVAILABILITY/LIMITATION NOTICES: Enter any limitations on further dissemination of the report, other than those imposed by security classification, using standard statements such as:

(1) "Qualified requesters may obtain copies of this report from DDC."

(2) "Foreign announcement and dissemination of this report by DDC is not authorized."

(3) "U. S. Government agencies may obtain copies of this report directly from DDC. Other qualified DDC users shall request through _____."

(4) "U. S. military agencies may obtain copies of this report directly from DDC. Other qualified users shall request through _____."

(5) "All distribution of this report is controlled. Qualified DDC users shall request through _____."

If the report has been furnished to the Office of Technical Services, Department of Commerce, for sale to the public, indicate this fact and enter the price, if known.

11. SUPPLEMENTARY NOTES: Use for additional explanatory notes.

12. SPONSORING MILITARY ACTIVITY: Enter the name of the departmental project office or laboratory sponsoring *(paying for)* the research and development. Include address.

13. ABSTRACT: Enter an abstract giving a brief and factual summary of the document indicative of the report, even though it may also appear elsewhere in the body of the technical report. If additional space is required, a continuation sheet shall be attached.

It is highly desirable that the abstract of classified reports be unclassified. Each paragraph of the abstract shall end with an indication of the military security classification of the information in the paragraph, represented as *(TS)*, *(S)*, *(C)* or *(U)*

There is no limitation on the length of the abstract. However, the suggested length is from 150 to 225 words.

14. KEY WORDS: Key words are technically meaningful terms or short phrases that characterize a report and may be used as index entries for cataloging the report. Key words must be selected so that no security classification is required. Identifiers, such as equipment model designation, trade name, military project code name, geographic location, may be used as key words but will be followed by an indication of technical context. The assignment of links, rules, and weights is optional

UNCLASSIFIED

Security Classification